Nitric-oxide synthase trafficking inducer is a pleiotropic regulator of endothelial cell function and signaling

Received for publication, June 8, 2016, and in revised form, February 22, 2017 Published, Papers in Press, February 24, 2017, DOI 10.1074/jbc.M116.742627

Shreeta Chakraborty[1] **and Rupasri Ain**[2]

From the Division of Cell Biology and Physiology, Council of Scientific and Industrial Research (CSIR)-Indian Institute of Chemical Biology, Kolkata 700032, West Bengal, India

Edited by Alex Toker

Endothelial nitric-oxide synthase (eNOS) and its bioactive product, nitric oxide (NO), mediate many endothelial cell functions, including angiogenesis and vascular permeability. For example, vascular endothelial growth factor (VEGF)-mediated angiogenesis is inhibited upon reduction of NO bioactivity both *in vitro* and *in vivo*. Moreover, genetic disruption or pharmacological inhibition of eNOS attenuates angiogenesis during tissue repair, resulting in delayed wound closure. These observations emphasize that eNOS-derived NO can promote angiogenesis. Intriguingly, eNOS activity is regulated by nitric-oxide synthase trafficking inducer (NOSTRIN), which sequesters eNOS, thereby attenuating NO production. This has prompted significant interest in NOSTRIN's function in endothelial cells. We show here that NOSTRIN affects the functional transcriptome of endothelial cells by down-regulating several genes important for invasion and angiogenesis. Interestingly, the effects of NOSTRIN on endothelial gene expression were independent of eNOS activity. NOSTRIN also affected the expression of secreted cytokines involved in inflammatory responses, and ectopic NOSTRIN overexpression functionally restricted endothelial cell proliferation, invasion, adhesion, and VEGF-induced capillary tube formation. Furthermore, NOSTRIN interacted directly with TNF receptor-associated factor 6 (TRAF6), leading to the suppression of NFκB activity and inhibition of AKT activation via phosphorylation. Interestingly, TNF-α-induced NFκB pathway activation was reversed by NOSTRIN. We found that the SH3 domain of NOSTRIN is involved in the NOSTRIN-TRAF6 interaction and is required for NOSTRIN-induced down-regulation of endothelial cell proteins. These results have broad biological implications, as aberrant NOSTRIN expression leading to deactivation of the NFκB pathway, in turn triggering an anti-angiogenic cascade, might inhibit tumorigenesis and cancer progression.

Angiogenesis is central to various physiological processes such as fetal growth, reproduction, wound healing, tissue repair (1). It is tightly regulated in a spatiotemporal manner by various angiogenic and anti-angiogenic factors, extracellular matrix components primarily derived from endothelial cells. Dysregulated angiogenesis either leads to or is associated with various pathological conditions such as tumorigenesis, cancer progression, vascular insufficiency in myocardial or critical limb ischemia, vascular overgrowth in hemangiomas, vascularized tumors, and retinopathies, among others (2). Thus, the identification of regulatory mechanisms and subsequent manipulation of angiogenesis will lead to numerous therapeutic opportunities to treat various pathological conditions.

Angiogenesis is a multistep process that includes the activation of endothelial cells followed by their proliferation, invasion into basement membrane matrix, capillary tube formation, and vessel stabilization (3). Vascular endothelial growth factor (VEGF) is a potent angiogenic factor and is up-regulated under various physiological and pathological angiogenic conditions (4). Another important pro-angiogenic factor is eNOS[3]-derived NO (5, 6). The pathophysiological conditions associated with hypertension and the reduced availability of NO are often accompanied by inhibition of angiogenesis (7).

NOSTRIN was initially discovered and characterized as an eNOS-sequestering protein. Overexpression of NOSTRIN in CHO cells stably transfected with eNOS (CHO-eNOS) led to the redistribution of eNOS from plasma membrane to vesicle structures with an almost 62% reduction in NO release. NOSTRIN was found to be abundantly expressed in highly vascularized tissues and was moderately expressed in HUVECs (8). Mouse NOSTRIN was cloned and characterized by Choi *et al.* (9) and was found to be expressed by retinoic acid-treated F9 teratocarcinoma cell line where eNOS was absent, indicating an eNOS-independent unexplored function of NOSTRIN. NOSTRIN is well-conserved in eukaryotes. Mouse and rat orthologs share an 81–82% sequence identity with human protein. It was further demonstrated that NOSTRIN interacts with caveolin-1 along with eNOS and forms a ternary complex asso-

This work was supported by Grant BT/PR9113/MED/97/134/2013 from the Department of Biotechnology, India; Grant 2012-0524 from the Indian Council of Medical Research; and Grant SB/SO/AS-114/2012 from the Department of Science and Technology, Council of Scientific and Industrial Research, India, in the form of network Projects BSC 0101 and BSC 0206. The authors declare that they have no conflicts of interest with the contents of this article.

This article contains supplemental Tables S1 and S2.

[1] Recipient of a predoctoral fellowship from the University Grant Commission, India.

[2] To whom correspondence should be addressed: Division of Cell Biology and Physiology, CSIR-Indian Institute of Chemical Biology, 4, Raja S. C. Mullick Rd., Jadavpur, Kolkata 700032, West Bengal, India. Tel.: 91-033-24995876; E-mail: rupasri@iicb.res.in.

[3] The abbreviations used are: eNOS, endothelial nitric-oxide synthase; NOSTRIN, nitric-oxide synthase trafficking inducer; HUVEC, human umbilical vein endothelial cell; qRT-PCR, quantitative real-time PCR; L-NNA, Nω-nitro-L-arginine; MTT, 3-(4,5-dimethylthiazol-2-yl)-2,5-diphenyltetrazolium bromide; ECM, extracellular matrix; TRAF, TNF receptor-associated factor; RTK, receptor tyrosine kinase.

ciated with decreased eNOS activity in CHO-eNOS cells overexpressing NOSTRIN. In HUVECs, stimulation by thrombin was required for the formation of the ternary complex (10). Another report, by Xu *et al.* (11), demonstrates that overexpression of NOSTRIN in HUVECs leads to a decrease in NO production. NOSTRIN has been shown to oligomerize to trimers in lysates of COS cells overexpressing GST-NOSTRIN using a gel filtration assay. In CHO-eNOS cells, NOSTRIN interacts with N-WASP and dynamin by overexpressing these proteins (12). It has been predicted that multiple proteins (eNOS, N-WASP, and dynamin) may interact with NOSTRIN via the SH3 domain due to the formation of the NOSTRIN oligomer. The N-terminal FCH domain of NOSTRIN is involved in membrane association in CHO-eNOS cells (13). Treatment of bovine pulmonary arterial endothelial cells with monocrotaline pyrrole, which is known to induce pulmonary hypertension in rats, leads to elevated NOSTRIN along with eNOS sequestration in cytoplasmic compartments and a complete loss of cell surface NO production (14). NOSTRIN expression is suppressed by a decrease in phopho-STAT3 in polyoma virus middle T-antigen-immortalized PECAM-1-KO endothelial cells along with an increase in eNOS activity and elevated NO production (15).

Thus, the existing literature using purified NOSTRIN and various deletion constructs in non-endothelial cells shows that NOSTRIN primarily decreases NO production and eNOS activity, which suggests that elevated NOSTRIN levels *in vivo* might lead to vasoconstriction and hypertension. In agreement with these *in vitro* studies, NOSTRIN protein levels were found to be significantly up-regulated in placentas and umbilical vessels of women with pre-eclampsia and pregnancy-induced hypertension with a reduction in NO production and eNOS activity (16–18). NOSTRIN levels were reported to be low in the testis of azoospermic patients with concomitant increase in eNOS activity and NO production (19). In addition, NOSTRIN was up-regulated in the liver of patients with alcoholic hepatitis/cirrhosis, known to be associated with portal hypertension (20). In these patients, a shorter variant of NOSTRIN (NOSTRIN-β) was expressed along with the full form of NOSTRIN (NOSTRIN-α). NOSTRIN-β lacks the N-terminal FCH domain and localizes to the nucleus. NOSTRIN-β was shown to bind to the 5′-regulatory region of the NOSTRIN gene using gel shift and luciferase assays (21). In mouse, *Nostrin* is present in both the nucleus and cytoplasm and represses its own promoter (22, 23).

Morpholino-mediated knockdown of *nostrin* in developing zebrafish embryos resulted in edema and hemorrhaging in the hindbrain and pericardial regions, indicating a malfunction of the vascular system. This phenotype can be reversed by *Nostrin* mRNA injection. In addition, filopodial extension in endothelial tip cells can be reduced in NOSTRIN morphants (24). Postnatal retinal angiogenesis was compromised in NOSTRIN-KO mice as compared with wild type. Those authors have further demonstrated a decrease in endothelial cell proliferation in the vascular front of the retina using Ki67 staining. In addition, the angiogenic response to FGF-2 using an *in vivo* Matrigel plug assay is compromised in NOSTRIN-KO mice. FGF-2 stimulus is mandatory in mouse lung endothelial cells for NOSTRIN interaction with FGFR1 (shown by co-immunoprecipitation) and subsequent increase in RAC1 activation (24). Another group has demonstrated, using morpholino-mediated knockdown of NOSTRIN in zebrafish, that NOSTRIN deficiency results in the effacement of podocyte foot processes and swelling of glomerular endothelial cells, whereas the tubular cell structure remains normal, as demonstrated by ultrastructural studies. This phenotype was associated with enhanced clearance of serum protein (25). The NOSTRIN and Cip4 double mutant in *Drosophila* exhibits increased formation of tubular E-cadherin vesicles at adherens junctions, although NOSTRIN and Cip4 do not hetero-oligomerize (26).

Interestingly, the group that discovered NOSTRIN has demonstrated its eNOS sequestering and NO release attenuation property (8, 10, 12, 13, 15, 20, 21). They also generated the NOSTRIN-KO mice and show that NOSTRIN is pro-angiogenic in a KO mouse model (24) and further report that endothelial cell-specific NOSTRIN-KO mice are characterized by impaired NO production in serum, hypertension, and diastolic cardiac dysfunction. This result not only contradicts their previous results of decreased eNOS activity by NOSTRIN but also disputes the finding of elevated NOSTRIN levels associated with hypertension in pregnancy-induced hypertension and pre-eclampsia patients (16–18). Moreover, a search for prognostic and predictive biomarkers of pancreatic ductal adenocarcinoma using 466 patient samples showed that increased NOSTRIN expression was associated with increased survival of patients, indicating an anti-angiogenic potential of NOSTRIN (27). Recently, NOSTRIN has been demonstrated as a negative regulator of disease aggressiveness in pancreatic cancer patients along with enhanced sensitivity to gemcitabine drug on NOSTRIN overexpression in human pancreatic cancer cell lines (28). It is, therefore, evident from the literature that the role of elevated levels of NOSTRIN in pathophysiological conditions such as pregnancy-induced hypertension, pre-eclampsia, and cancer progression is different from the phenotypes exhibited by NOSTRIN KO mice and the zebrafish model. Moreover, a very mild postnatal pro-angiogenic phenotype in NOSTRIN KO mice indicates overcompensation of NOSTRIN function by other F-BAR proteins. Taking together these contradictory reports, the mechanism of elevated NOSTRIN function in endothelial cells under pathophysiological conditions needs to be explored. Interestingly, we found that NOSTRIN expression gradually increases during uteroplacental development in mice, and it shows a reciprocal expression pattern with eNOS.[4] In the same line, NOSTRIN was also found in F9 mouse teratocarcinoma cells where eNOS was not detected (9). These result led us to hypothesize that NOSTRIN might have some important yet unexplored function in endothelial cells that is independent of eNOS. Murine endothelial cell line MS1 is known to form angiosarcomas *in vivo* (29–31). Thus to elucidate the function of NOSTRIN in a pathophysiological context, we investigated the endogenous biological role of NOSTRIN in MS1 endothelial cells.

[4] S. Chakraborty and R. Ain, unpublished data.

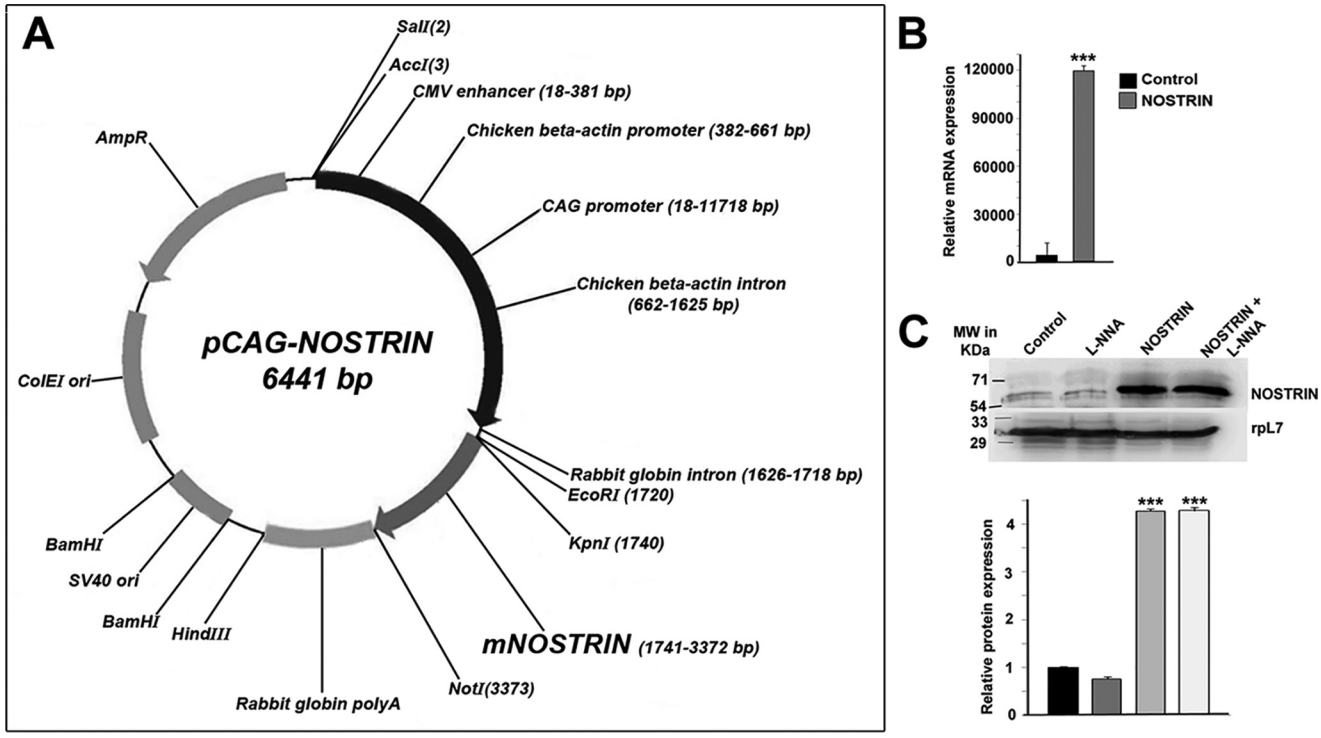

Figure 1. Overexpression of *Nostrin* in MS1 endothelial cells. *A*, mammalian expression vector containing full-length *Nostrin* cDNA cloned from murine placenta under synthetic CAG promoter. *B*, overexpression of full-length *Nostrin* in MS1 endothelial cells by transfection of pCAG-NOSTRIN was quantified by real-time PCR, and a massive up-regulation in mRNA transcript was obtained. In each experiment requiring *Nostrin* overexpression, up-regulation of *Nostrin* was confirmed by real-time PCR. *C*, Western blotting analysis of NOSTRIN. The four treatment groups included were endothelial cells transfected with vector backbone (*Control*), vector backbone along with L-NNA treatment, *Nostrin* cDNA, and *Nostrin* cDNA followed by L-NNA treatment. The experiments were repeated using at least three independent biological replicates. *rpL7* was used as a loading control. Quantification of protein bands is show in the *bar graph* (*lower panel*), normalized to the loading control using ImageJ software. Values are represented as mean ± S.E. of three independent experiments. ***, $p < 0.005$ (*B* and *C*).

Results

Functional transcriptome analysis reveals the importance of NOSTRIN in regulating endothelial cell biology

The most prominent function of NOSTRIN that has been reported to date is the sequestering of eNOS within intracellular vesicular structures and rendering it inactive, thus reducing the NO levels. Our hypothesis on the eNOS-independent function of NOSTRIN prompted us to analyze NOSTRIN function in endothelial cells. To elucidate the transcriptional targets dependent on NOSTRIN expression, we performed a real-time PCR-based mouse endothelial cell biology RT^2 Profiler array, comparing endothelial cells expressing control vector *versus* cells overexpressing *Nostrin* cDNA (Fig. 1*A*). Elevated levels of *Nostrin* mRNA and protein were confirmed by real-time PCR and Western blotting, respectively, in endothelial cells ectopically overexpressing NOSTRIN (Fig. 1, *B* and *C*). Eighty-four genes related to various endothelial cell functions such as endothelial cell activation, permissibility, vascular tone, angiogenesis, and endothelial cell injury were analyzed (Fig. 2, *A* and *B*). Overall, 68 transcripts met the recommended cutoff readings ($C_t \leq 30$) in at least one of the two groups (supplemental Table S1). Of these, 32 transcripts were changed significantly (2-fold or greater, $p < 0.05$) between two groups in the array. Twenty-eight genes related to the modulation of vascular tone, invasion, extracellular matrix remodeling, and angiogenesis were down-regulated (Table 1). In addition, ectopic overexpression of *Nostrin* also led to down-regulation of secreted pro-inflammatory cytokines *IL6*, *Ccl2*, and *Ccl5*. In contrast, expression of *Edn1*, a potent vasoconstrictor, was up-regulated upon overexpression of NOSTRIN (Fig. 2, *A* and *B*). siRNA-mediated down-regulation of NOSTRIN in endothelial cells was done to complement the experimental findings obtained by ectopic overexpression of NOSTRIN. Two prevalidated Silencer Select siRNAs that target the NOSTRIN coding regions were used for these experiments. The optimum concentration of individual siRNAs was determined by a dose-response curve. A dosage of 20 nM total siRNA (10 nM each) yielded a maximum down-regulation of *Nostrin* by 82% as compared with the other dosages used, such as 100 and 200 nM (Fig. 2*D*). This concentration was used in further down-regulation experiments. A similar PCR-based array was performed to screen 84 endothelial function-associated genes in NOSTRIN-down-regulated endothelial cells compared with control cells transfected with scrambled siRNA (Fig. 2, *E* and *F*). There was an overall up-regulation of genes that were down-regulated on ectopic overexpression of NOSTRIN. However, the changes in threshold values or -fold regulation were not as high as those obtained for overexpression. Although most of the genes displayed the expected reciprocal response in up- and down-regulated NOSTRIN cells, there were some apparent discrepancies in wells A01, A12, B04, B06, B07, B11, B12, C01, C10, D12, E01, E05, E07, E08, F10, G05, and G012 (Fig. 2, *A* and *E*). A critical anal-

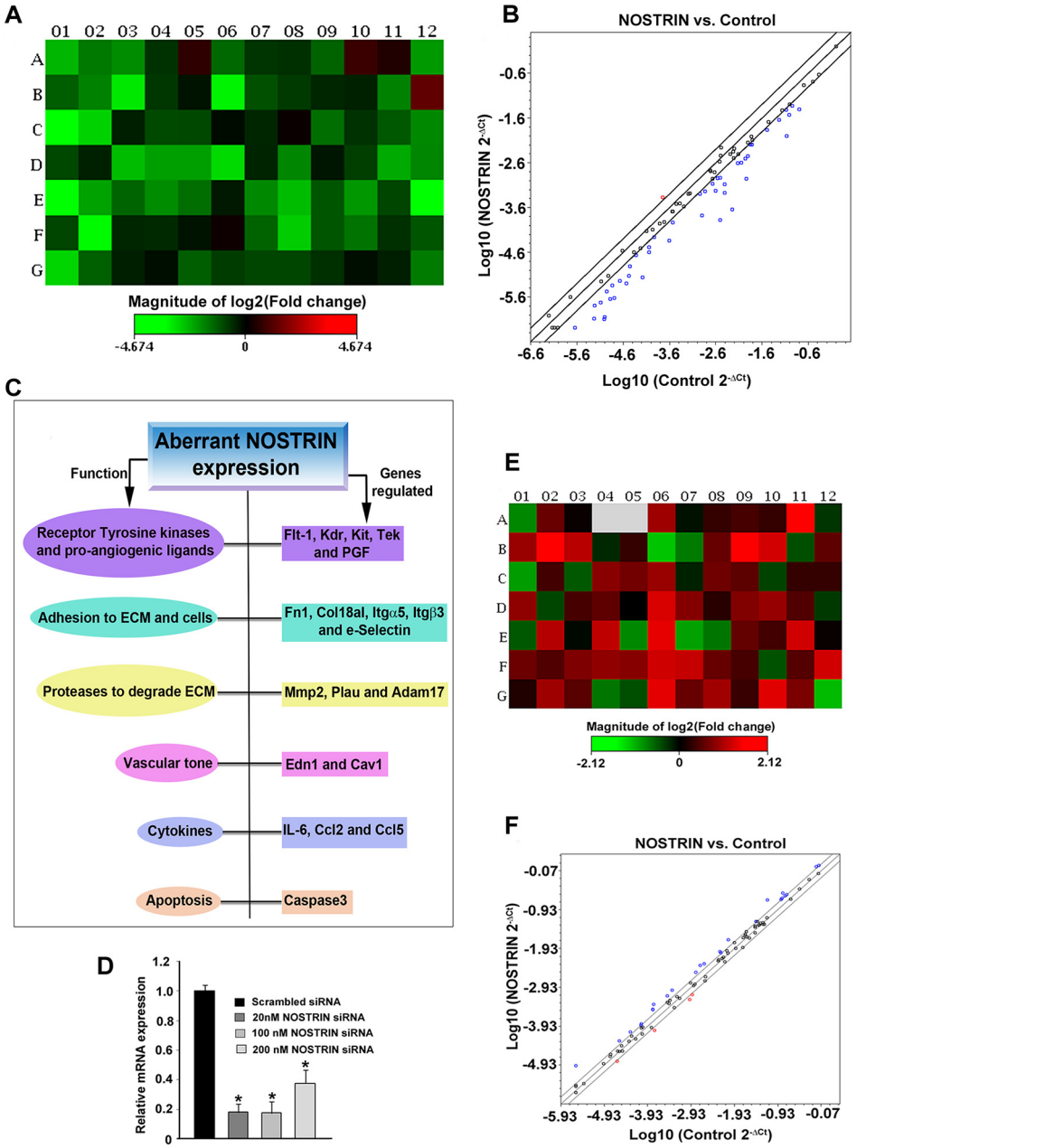

Figure 2. PCR array analysis profiling the functional transcriptome of endothelial cells by ectopic overexpression or siRNA-mediated down-regulation of *Nostrin*. *A*, heat map represents the fold change in expression of 84 different genes in *Nostrin*-overexpressing endothelial cells as compared with control cells transfected with empty vector backbone (see also Fig. 1, *A* and *B*). Normalization was done using the housekeeping gene, which showed no change in NOSTRIN-overexpressed MS1 cells compared with control in three biological replicates using online software provided by SABiosciences. Up-regulated genes are shown in *red*, down-regulated in *green*, and those not regulated in *black*. *B*, *scatter plot* shows genes with similar expression levels (within the *black lines*) that are close to the line of regression. The *red dots above* the *black lines* represent up-regulated genes, whereas the *blue dots below* the *lines* represent down-regulated genes. The *scatter plot* demonstrates the log10 of normalized gene expression levels in the control group (*x* axis) *versus* that in NOSTRIN-overexpressing condition (*y* axis). Values are represented as mean ± S.E. of three independent experiments. *C*, function-based annotation of the 19 genes that are differentially regulated in all three experiments. Results about aberrant *Nostrin* expression are shown in a flowchart. *D*, real-time PCR showing siRNA-mediated down-regulation of *Nostrin* using a combination of two prevalidated Silencer Select siRNAs at three different dosages. A 20 nM dose of total siRNAs (at 10 nM each) was used for further experiments. *E*, heat map representing the change in expression of 84 genes by PCR array using mRNA from NOSTRIN down-regulated (20 nM concentration) endothelial cells compared with scrambled siRNA treatment. *Colors* depicted in individual wells are analyzed similarly as described above in *A*. *F*, *scatter plot* of *Nostrin* down-regulation shows that most of the genes displayed similar expression levels (within *black lines*), and -fold change values were less than 1 (not significant). The graphs and plots were generated using the mean values of three biological replicates. *, $p < 0.05$ (*D*).

ysis showed that wells B11, C01, C10, E08, F10, and G12 had average threshold values of ≥30 in either of the data sets and, therefore, were not relevant. Wells A01, A12, B04, B06, B07, B12, D12, E01, E05, E07, and G05 had a -fold change of <1 (Fig. 2*F*) and hence were irrelevant. As per SABioscieces guidelines, genes screened from PCR arrays should have a minimum 2-fold change in all of the replicates; although a slight change in C_t value can give rise to the displayed color in the heat map, this might not be significant. It is also important to note here that endogenous expression levels of NOSTRIN in mouse MS1

Table 1

NOSTRIN-induced alteration of transcripts associated with endothelial cell function

Only the transcripts that changed significantly (2-fold or more, $p < 0.05$) between the control and the overexpressed group in the array are shown.

Serial No.	Gene symbol	Control C_t average	NOSTRIN C_t average	-Fold change	Gene description
1	*Ace*	26.38	28.55	−5.4514	Angiotensin I-converting enzyme (peptidyl-dipeptidase A) 1
2	*Adam17*	21.44	22.77	−3.0424	A disintegrin and metallopeptidase domain 17
3	*Anxa5*	18.47	19.59	−2.6115	Annexin A5
4	*Bcl2*	23.27	24.32	−2.4977	B-cell leukemia/lymphoma 2
5	*Casp3*	23.04	24.82	−4.1379	Caspase 3
6	*Cav1*	17.56	18.53	−2.3664	Caveolin 1, caveolae protein
7	*Ccl2*	17.76	19.2	−3.2802	Chemokine (C-C motif) ligand 2
8	*Ccl5*	17.93	20.77	−8.6405	Chemokine (C-C motif) ligand 5
9	*Col18a1*	28.28	31.25	−9.4839	Collagen, type XVIII, α1
10	*Edn1*	26.86	25.31	2.4132	Endothelin 1
11	*Fgf1*	27.82	29.02	−2.7709	Fibroblast growth factor 1
12	*Flt1*	24.16	25.07	−2.2661	FMS-like tyrosine kinase 1
13	*Fn1*	21.21	22.75	−3.5179	Fibronectin 1
14	*Il6*	24.03	26.68	−7.5833	Interleukin 6
15	*Itga5*	20.73	22.25	−3.4566	Integrin α5 (fibronectin receptor α)
16	*Itgβ3*	22.37	24.36	−4.7976	Integrin β3
17	*Kdr*	20.93	22.45	−3.4719	Kinase insert domain protein receptor
18	*Kit*	22.7	27	−23.700	Kit oncogene
19	*Mmp1a*	29.26	31.15	−4.4491	Matrix metallopeptidase 1a
20	*Mmp2*	26.1	27.18	−2.5489	Matrix metallopeptidase 2
21	*Mmp9*	29.92	31.53	−3.6915	Matrix metallopeptidase 9
22	*Nos3*	22.7	23.89	−2.7528	Nitric-oxide synthase 3, endothelial cell
23	*Npr1*	27.82	29.39	−3.5733	Natriuretic peptide receptor 1
24	*Pecam1*	17.04	18.8	−4.0806	Platelet/endothelial cell adhesion molecule 1
25	*Pgf*	21.83	26.24	−25.530	Placental growth factor
26	*Plau*	20.84	23.93	−10.282	Plasminogen activator, urokinase
27	*Sele*	23.81	24.88	−2.5229	Selectin, endothelial cell
28	*Selp*	20.56	21.41	−2.1812	Selectin, platelet
29	*Sod1*	17.96	18.82	−2.1893	Superoxide dismutase 1, soluble
30	*Tek*	22.39	24.98	−7.2576	Endothelial-specific receptor tyrosine kinase
31	*Tfpi*	22.9	23.9	−2.4146	Tissue factor pathway inhibitor
32	*Thbs1*	19.35	20.34	−2.3842	Thrombospondin 1

endothelial cells were low as determined by the high C_t value in quantitative real-time PCR (qRT-PCR) along with immunoblot analysis (Fig. 1, *B* and *C*). siRNA-mediated down-regulation led to a further increase in the C_t values beyond the cutoff recommended by Applied Biosystems (data not shown). Thus, down-regulation of NOSTRIN, although it complemented the overexpression data (Fig. 2), was not used for further experiments. We therefore used the overexpression of NOSTRIN for subsequent studies.

The differential expression of genes identified in the PCR array was further validated by qRT-PCR using *rpL7* as an endogenous control. Real-time primers used for the qRT-PCR are listed in supplemental Table S2. Nineteen of the 32 transcripts found in the array were truly differentially regulated by *Nostrin* overexpression in all the three replicate qRT-PCR experiments. The functional annotation of these 19 genes is summarized in Fig. 2*C*. These genes are broadly categorized into three groups. The first group of genes primarily regulates invasion, adhesion, and angiogenesis. These included the receptor tyrosine kinases, (*Kdr*, *Flt-1*, *Kit*, and Tek) and the pro-angiogenic ligand of *Flt-1*, *i.e. Pgf* (Fig. 3*A*), adhesion genes (*Fn1*, *Col18a1*, *Itgβ3*, *Itgα5*, and *Sele*) (Fig. 3*B*), and proteases (*Plau*, *Mmp-2*, and *Adam-17*) (Fig. 3*C*). Genes belonging to these groups were all significantly ($p < 0.01$ or 0.005) down-regulated. The second group comprises genes that regulate vascular tone, which include *Edn1* and *Cav1*. Interestingly, *Edn1* was up-regulated, whereas *Cav1* expression decreased, (Fig. 3*D*) upon *Nostrin* overexpression. The third group of genes involved the chemokines and cytokines that regulate inflammation. *IL6*, *Ccl2*, and *Ccl5* belong to this category, and mRNA expression of these genes was down-regulated on NOSTRIN overexpression (Fig. 3*E*). In addition, *Casp3* expression was also reduced on NOSTRIN overexpression (Fig. 3*F*).

NOSTRIN down-regulates endothelial cell functional proteins independent of its effect on eNOS

Because mRNA levels do not always correlate with the corresponding protein abundance, for a better interpretation of our transcriptome analysis, we evaluated the protein levels either by immunoblot assay or ELISA. Furthermore, we also investigated whether the influence of NOSTRIN on endothelial cell protein levels is NOS-dependent, as NOSTRIN is classically known to sequester eNOS.

First, we examined the effect of NOSTRIN on nitric oxide production, which is known to be the product of eNOS in endothelial cells. Inhibition of NOS by Nω-nitro-L-arginine (L-NNA) led to an 82% decrease in NO production in endothelial cells. NOSTRIN overexpression reduced the NO levels by 34% in unstimulated endothelial cells. The cumulative effect of inhibition of NOS along with NOSTRIN overexpression led to complete attenuation (by 98%) of endogenous NO production (Fig. 4*A*). Phospho-eNOS and total eNOS levels were assessed by Western blotting analysis in four treatment groups. Cells transfected with vector backbone were treated with either vehicle (control) or L-NNA. *Nostrin* cDNA-transfected cells were treated similarly. Quantification of phosphorylated eNOS levels at Ser-1177 showed that NOSTRIN overexpression did not affect phospho-eNOS or total eNOS protein levels. However, there was a significant ($p < 0.01$) reduction of phospho-eNOS levels in L-NNA-treated endothelial cells, both in the absence and presence of NOSTRIN (Fig. 4, *B* and *C*). These data indicate

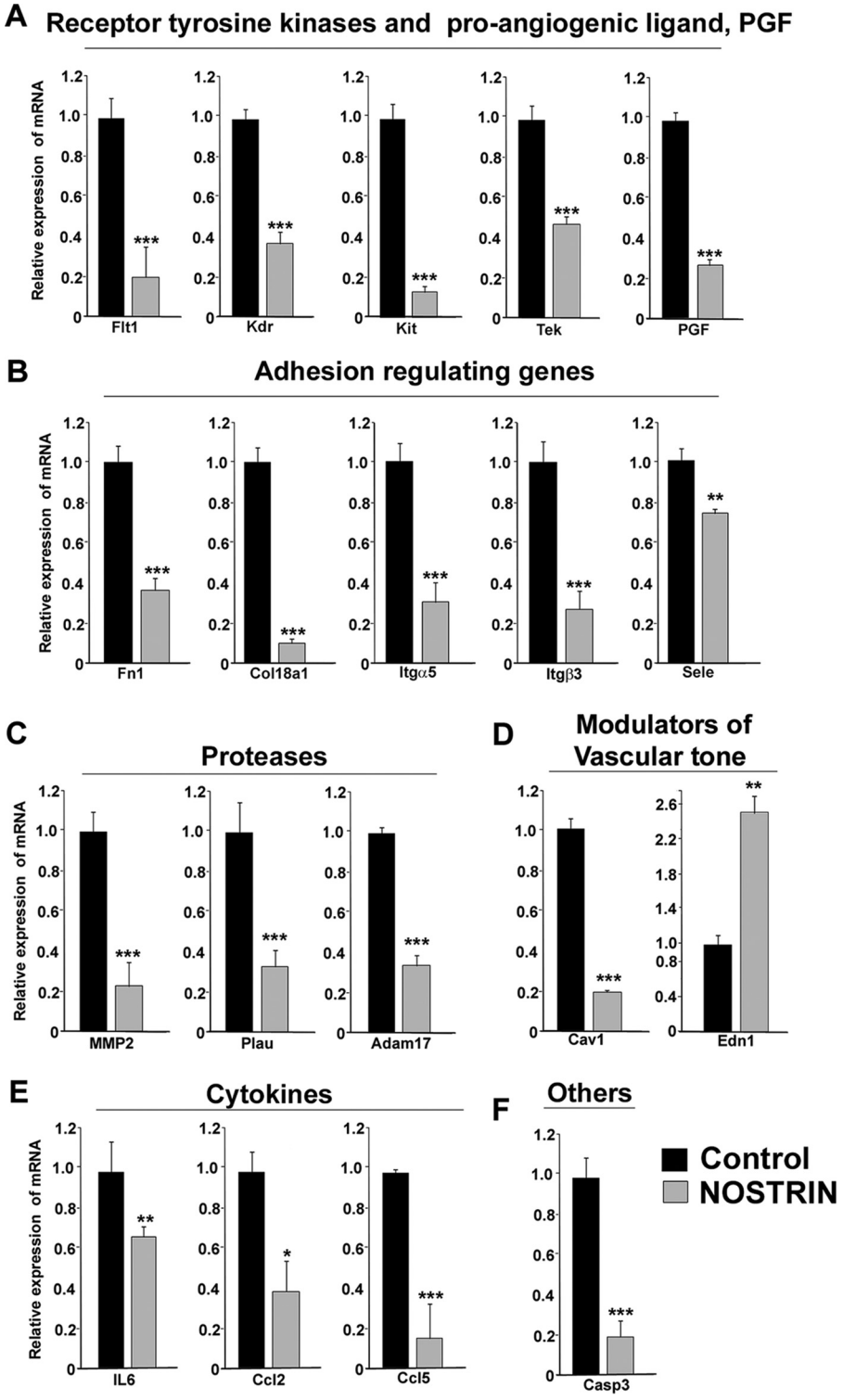

Figure 3. Real-time PCR analysis of transcripts in endothelial cells affected by aberrant NOSTRIN expression. Quantitative real-time PCR analysis of endothelial function-associated genes shows significant differences in *Nostrin*-overexpressed *versus* control endothelial cells. The amount of a specific mRNA was normalized relative to the amount of rpL7 ($\Delta C_t = C_{tgene} - C_{trpL7}$). The -fold change of gene expression was measured by using $2^{-\Delta\Delta C}{}_t$, where $\Delta\Delta C_t$ denotes the change in ΔC_t values between samples and reference sample (here, vector backbone-transfected endothelial cells sample was used as the reference sample, $\Delta\Delta C_t = \Delta C_{tgene\_NOSTRIN} - \Delta C_{tgene\_control}$). *Error bars* represent S.E. from three different biological replicates. *A*, the receptor tyrosine kinases including *Flt-1*, *Kdr*, *Kit*, and *Tek* along with the pro-angiogeneic ligand *Pgf*, which can bind to *Flt-1*, were down-regulated significantly with overexpression of NOSTRIN. *B*, NOSTRIN overexpression led to significant down-regulation of transcripts of several genes involved in adhesion and invasion such as *Fn1*, *Col18a1*, *Itgα5*, *Itgβ3*, and *Sele*. *C*, expression of the three proteases *Mmp-2*, *Plau*, and *Adam*-17 was found to be diminished remarkably by NOSTRIN overexpression. *D*, *Cav1*, a well-known regulator of vascular tone, was down-regulated, whereas *Edn-1*, a vasoconstrictor, was up-regulated significantly by NOSTRIN overexpression. *E*, a significant decrease in mRNA levels of cytokines such as *IL6*, *Ccl2*, and *Ccl5* was induced by NOSTRIN overexpression. *F*, *Casp3*, which induces apoptosis, was found to be down-regulated on NOSTRIN overexpression. *, $p < 0.05$; **, $p < 0.01$; and ***, $p < 0.005$.

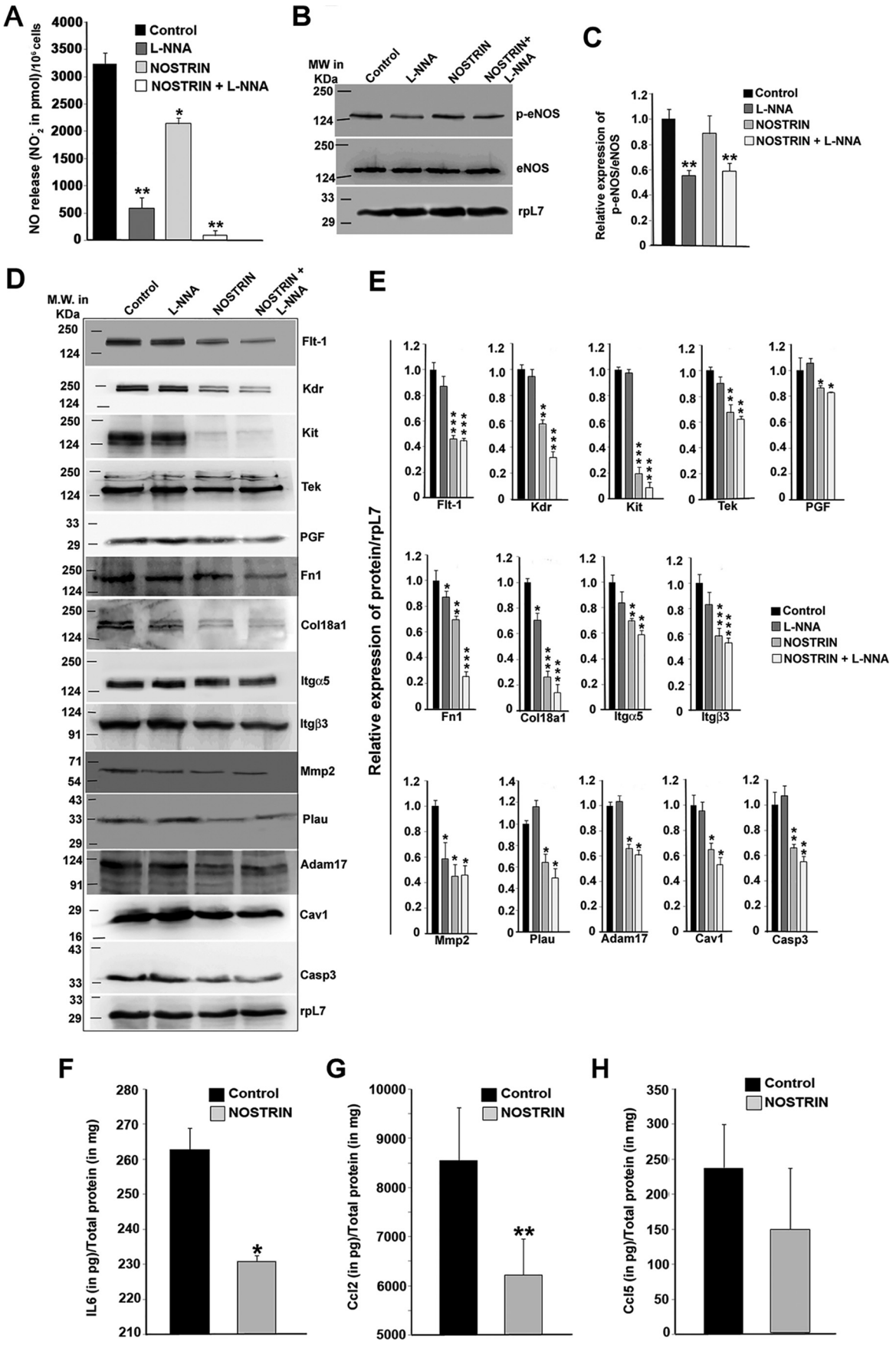
A
NO release (NO^-_2 in pmol)/10^6 cells
Control
L-NNA
NOSTRIN
NOSTRIN + L-NNA
B
MW in KDa
Control
L-NNA
NOSTRIN
NOSTRIN+ L-NNA
p-eNOS
eNOS
rpL7
C
Relative expression of p-eNOS/eNOS
D
M.W. in KDa
Flt-1
Kdr
Kit
Tek
PGF
Fn1
Col18a1
Itgα5
Itgβ3
Mmp2
Plau
Adam17
Cav1
Casp3
rpL7
E
Relative expression of protein/rpL7
F
IL6 (in pg)/Total protein (in mg)
G
Ccl2 (in pg)/Total protein (in mg)
H
Ccl5 (in pg)/Total protein (in mg)

that the phosphorylation of eNOS is not affected by its binding to NOSTRIN. However, our data showed that phosphorylation of eNOS is affected by L-NNA. Previous reports also suggest that L-NNA can suppress eNOS phosphorylation mediated by PKA (32) or that it may involve an AMPK-dependent pathway (33).

Proteins corresponding to 16 of the 19 genes associated with endothelial cell function that were regulated by NOSTRIN were evaluated by immunoblot analysis using *rpL7* as an endogenous control. Three secreted proteins, IL6, CCL2, and CCL5, were evaluated by ELISA. Immunoblotting was done in four different treatment groups that included endothelial cells transfected with (*a*) vector backbone, (*b*) vector backbone along with L-NNA treatment, (*c*) *Nostrin* cDNA, and (*d*) *Nostrin* cDNA followed by L-NNA treatment. Concordant with mRNA regulation, NOSTRIN overexpression decreased the protein levels of all 14 of the genes (Fig. 4*D*). Densitometric analysis of the blots (Fig. 4*E*) showed that there was significant ($p < 0.05$, 0.01, or 0.005) reduction in the protein levels of all of the functional groups of genes described previously. On the other hand, NOS inhibition by L-NNA in the absence of NOSTRIN resulted in no significant change in the protein level of 11 genes and led to a slight decrease in the protein level of three of the genes. The receptor tyrosine kinases, which included FLT-1, KDR, KIT, and TEK, had no effect on NOS inhibition but were down-regulated in the presence of NOSTRIN as compared with control. Adhesion genes Itgα5 and Itgβ3 had almost similar expression levels as control on NOS inhibition, but *FN1* and COL18A1 showed a 15 and 30% decline in the protein level, respectively, which was further decreased in the presence of NOSTRIN (30 and 70% down-regulation, respectively). Proteolytic enzymes such as *PLAU* and *ADAM-17* were down-regulated only in the presence of NOSTRIN, whereas MMP2 protein levels were significantly ($p < 0.05$) decreased in all of the three treatment groups compared with control. Other functional proteins, such as PGF, CAV1, and CASP3, were significantly ($p < 0.05$) down-regulated on NOSTRIN overexpression but remained unaltered by L-NNA treatment. Expression of EDN1 and SELE did not show a significant change at the protein level (data not shown). The protein levels of secreted cytokine IL6 and chemokines such as CCL2 and CCl5 were determined by ELISA in endothelial cells transfected with empty vector or *Nostrin* cDNA (Fig. 4, *F–H*). IL6 and CCL2 were significantly ($p < 0.05$ and 0.01, respectively) down-regulated by NOSTRIN overexpression, whereas there was no significant change in the protein levels of CCL5.

NOSTRIN inhibits angiogenic potential of endothelial cells by abrogating multiple functions of endothelial cells required for angiogenesis

Angiogenesis is a multistep process, and cell proliferation is the earliest event that takes place following the activation of endothelial cells during the initiation of angiogenesis. To evaluate the effect of NOSTRIN on endothelial cell proliferation and to test whether this effect is NOS-dependent, we performed an MTT assay using four different treatment groups, as mentioned above. Inhibition of NOS in the presence of vector backbone led to a slight (10%) increase in cell proliferation. This result corroborates with previously published information on NO-mediated inhibition of cell growth and proliferation *in vitro* (34). NOSTRIN, however, effectively ($p < 0.05$) suppressed cell proliferation by 17%, and the presence of an NOS inhibitor along with NOSTRIN prevented NOS inhibition and led to a similar decline in cell proliferation by 15% (Fig. 5*A*). MTT assay results on cell proliferation were further substantiated by using a BrdU cell proliferation assay with the same treatment groups. Cell proliferation increased by 12% on NOS inhibition, whereas a 25% decrease in proliferation was observed by NOSTRIN overexpression even in the presence of L-NNA (Fig. 5*B*). These data show that the inhibitory effect of NOSTRIN on endothelial cell proliferation is independent of eNOS.

Following activation and proliferation, endothelial cells degrade the capillary wall by extracellular proteases followed by migration and invasion of endothelial cells into the extracellular matrix. As NOSTRIN overexpression led to a significant decrease in the mRNA and protein levels of invasion-related genes, we sought to investigate the effect of NOSTRIN on endothelial cell migration and invasion. A scratch wound assay was used to evaluate cell migration. Photomicrographic images depicting the wound at the time of scratching (0 h) and at 6, 12, 18, and 24 h post-wounding in cells from the four treatment groups are shown in Fig. 5*C*. Following scratch wounding, cells expressing the control vector migrated into the wound and closed nearly 74% of it by 24 h. Wound closure of cells treated with L-NNA, after 24 h was 62%. In contrast, cells overexpressing NOSTRIN were remarkably sluggish in their ability to close the wound site, and only 37% of the wound was closed by the NOSTRIN-overexpressing cells. Similar results were obtained using cells overexpressing NOSTRIN and treated with NOS inhibitor, wherein only 30% of the wound was closed by 24 h (Fig. 5*D*). These data indicate that cells overexpressing NOSTRIN markedly attenuate the migration potential of endothelial cells and that this function is eNOS-independent.

Figure 4. NOSTRIN decreases NO levels in endothelial cells without affecting the phopho-eNOS levels, and the effect of NOSTRIN on endothelial cell function-associated proteins is eNOS-independent. *A*, NO production was measured in culture supernatants in the form of nitrites. *Error bars* represent S.E. from three different biological replicates. *B*, Western blotting analysis of eNOS and phospho-eNOS from endothelial cells from the four treatment groups. *C*, relative expression of phospho-eNOS with respect to eNOS was quantified by ImageJ software after normalization with rpL7 using three biological replicates from *B*. *D*, Western blotting analysis of protein levels of 14 of 19 genes, associated with various endothelial cell functions were reproducibly altered by NOSTRIN overexpression in three biological replicates. The positions of the molecular-weight markers for the spliced blots are shown on the *left* side of the image. *E*, quantification by ImageJ software of the proteins relative to rpL7 using three biological replicates from *D*. *F–H*, ELISA analysis of secreted cytokines from endothelial cells transfected with NOSTRIN and vector backbone (*Control*). Cytokines were quantified in pg relative to total protein estimated in mg. Each experiment was repeated three times with different biological samples. *Error bars* represent S.E. *, $p < 0.05$; **, $p < 0.01$; and ***, $p < 0.005$.

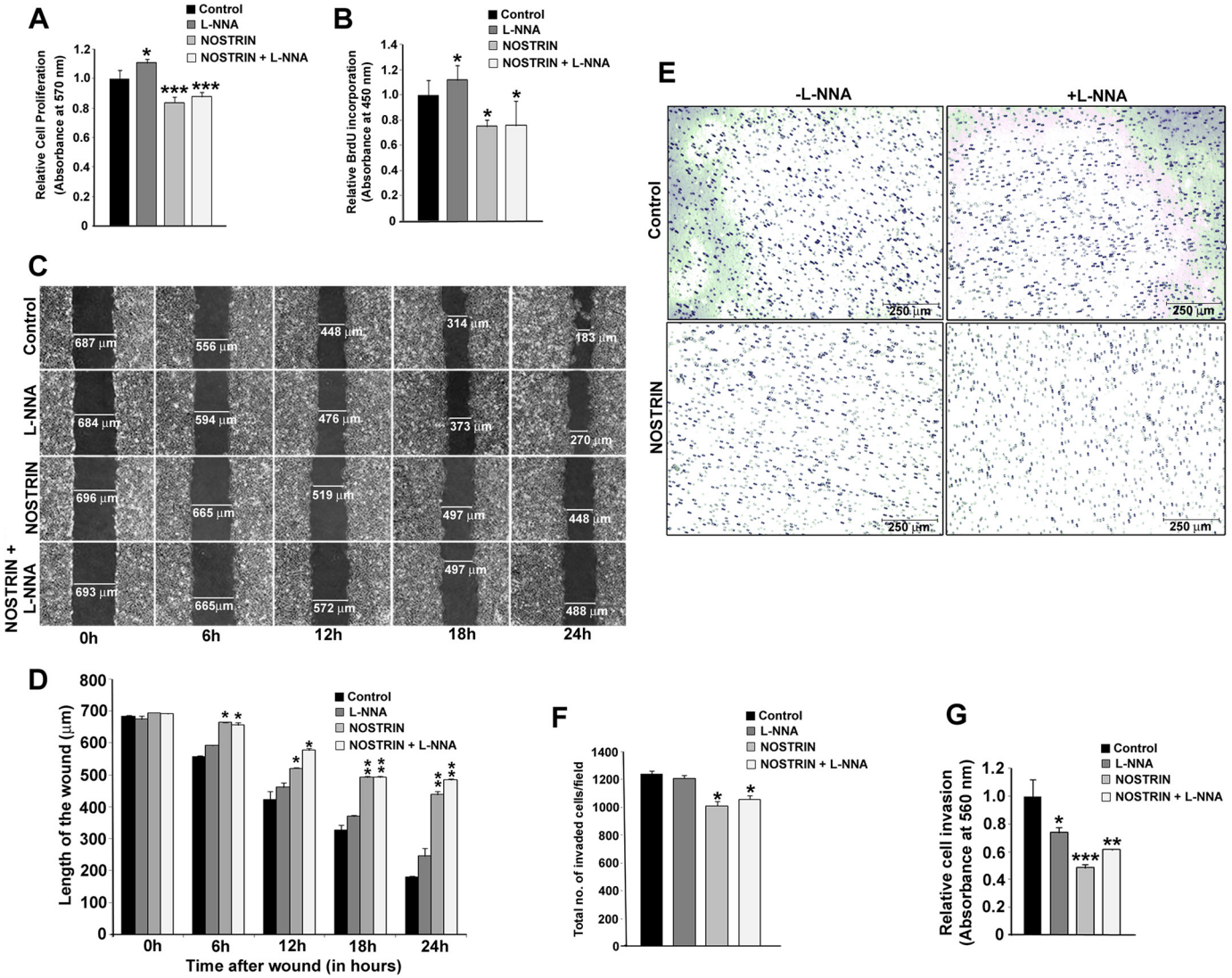

Figure 5. NOSTRIN curtails the angiogenic potential of endothelial cells by inhibiting cell proliferation, migration and invasion. *A*, MTT assay showing NOSTRIN-mediated repression of endothelial cell proliferation. The four treatment groups are the same as described in the legend for Fig. 4. *Error bars* represent S.E. from three different biological replicates. *B*, BrdU incorporation assay demonstrating inhibition of cell proliferation by NOSTRIN. *Error bars* represent S.E. from three different biological replicates. *C*, photomicrographic images from the scratch wound assay depicting wound closure at various time points in the four treatment groups. *D*, quantification by Leica LAS software of the length of the wound at various time intervals from a minimum of five measurements in each experiment using three different biological samples. At each time point, the length of the wound was compared with that of control. Starting from 6 h, the length of the wound was significantly bigger in the presence of NOSTRIN as compared with control. *E*, photomicrograph of invaded endothelial cells from the cell invasion assay. *F*, cell count per microscopic field from the four treatment groups. *Error bars* represent S.E. calculated using values of the count from three different biological replicates and five microscopic fields per replicate. *G*, colorimetric quantification of the stained, invaded cells at the lower surface of the membrane in the four treatment groups. *Error bars* represent S.E. from three biological replicates. *, $p < 0.05$; **, $p < 0.01$; and ***, $p < 0.005$.

A similar inhibitory role of NOSTRIN was observed on endothelial cell invasion toward chemoattractant. For these experiments, cells were plated on Transwell inserts precoated with extracellular matrix (ECM) proteins, collagen, and elastin. The ability of cells to invade the matrix and attach to the underside of the Transwell membrane was scored as well as quantified. Representative photomicrophaphic images of stained cells on the underside of the Transwell are shown in Fig. 5*E*. The total number of cells was counted in all four treatment groups in three biological replicates. At least five fields/well were counted, and the average cell count/field is shown in Fig. 5*F*. There was a significant ($p < 0.05$) decrease of ~19% in the total cell count of invaded cells under NOSTRIN-overexpressing conditions and only a 2% decrease when NOS was inhibited (Fig. 5*F*). Colorimetric quantification of the stained invaded cells also showed that there was a 51% reduction in the absorbance in NOSTRIN-overexpressing cells as compared with the control, indicating that invasion was severely affected by NOSTRIN (Fig. 5*G*). Inhibition of NOS by L-NNA in the absence of NOSTRIN led to a 26% decrease in absorbance, and in the presence of NOSTRIN absorbance was diminished by 39%.

The formation of new branch points, as well as the interconnection of new tubes to form a network, is a hallmark of angiogenesis. This process is mimicked *ex vivo* by VEGF-induced capillary tube formation by endothelial cells on Matrigel substrates. We used this assay to evaluate the effect of NOSTRIN on endothelial cell tube formation ability. Following plating on

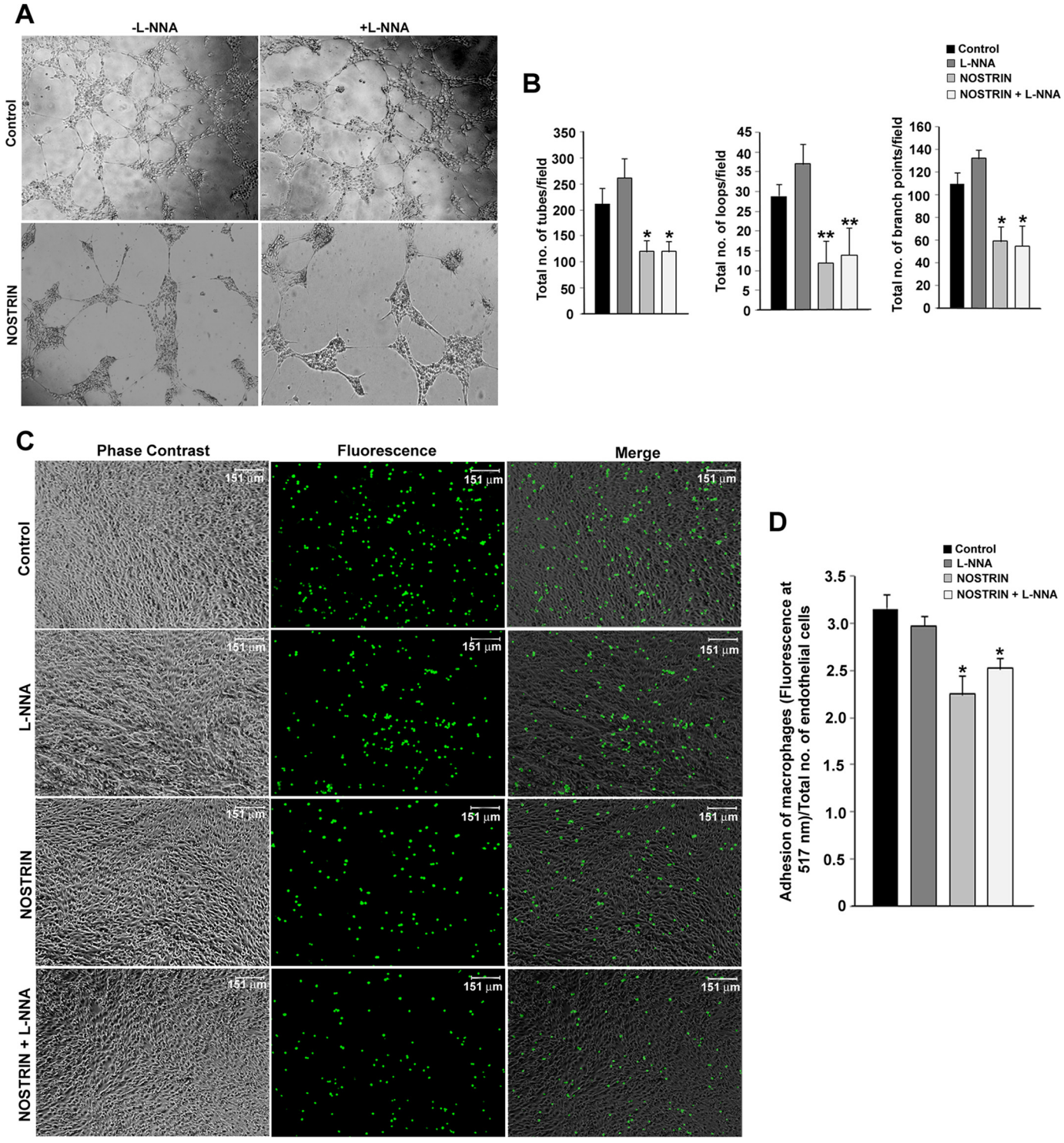

Figure 6. NOSTRIN inhibits VEGF-induced tube formation and adhesion of macrophages to endothelial cells. *A*, photomicrograph of tube formation in the four treatment groups at 12 h following plating of cells on basement membrane matrix-coated plates. Experiments were repeated three times with different biological samples. *B*, quantification of capillary tube formation in four treatment groups using data from three replicate experiments and five random microscopic fields per experiment. Data were analyzed using Wimasis image analysis software. *Error bars* represent S.E. *C*, photomicrograph images of calcein-labeled macrophages adhered to endothelial cell monolayer from four treatment groups. *D*, quantification of fluorescence of the adhered macrophages normalized to total number of endothelial cells available per well. *, $p < 0.05$; and **, $p < 0.01$.

Matrigel, endothelial cells transfected with empty vector or cells treated with NOS inhibitor formed networks of tubes. However, cells overexpressing NOSTRIN were unable to efficiently form tubes but rather formed tight clusters that inefficiently connected to adjacent clusters. The addition of L-NNA to NOSTRIN-overexpressing cells did not affect tube formation. Photomicrographic images of tube formation in these four different groups are shown in Fig. 6*A*. The quantification of tube formation was done using three criteria: number of tubes, number of loops, and number of branch points.

NOSTRIN overexpression led to a 43% reduction in the number of tubes, a 58% reduction in the number of loops, and a 46% reduction in the number of branch points as compared with controls. The addition of L-NNA alone in the absence of NOSTRIN did not have any inhibitory effect on tube formation (Fig. 6*B*).

Influence of NOSTRIN on adhesion of macrophages to endothelial cell monolayer

NOSTRIN-mediated down-regulation of several cell adhesion molecules such as ITGβ3, ITGα5, and FN1, as well as the down-regulation of proinflammatory cytokine and chemokines, led us to investigate the effect of NOSTRIN on adhesion of macrophages on endothelial cell monolayer using four treatment groups. The adherence of calcein-labeled RAW264.7 macrophages was not affected by L-NNA treatment, whereas NOSTRIN overexpression diminished macrophage adhesion to endothelial cells as compared with control. L-NNA treatment of NOSTRIN-overexpressing cells did not further potentiate the adhesion of macrophages (Fig. 6*C*). Fluorometric quantification of adhered macrophages/endothelial cell showed that there was a significant ($p < 0.05$) reduction of 29% in the adhesion of macrophages to NOSTRIN-overexpressing endothelial cells as compared with control. Cell adhesion was reduced by 20% in L-NNA-treated NOSTRIN-overexpressing cells (Fig. 6*D*). As expected, NOS inhibition alone in vector-transfected cells did not show a significant change as compared with control.

These experiments assessing the influence of NOSTRIN on various functions of endothelial cells corroborate the effect of NOSTRIN on the functional transcriptome of endothelial cells. These functional data prove the anti-angiogenic potential of NOSTRIN-independent of eNOS activity.

NOSTRIN down-regulates the NFκB-signaling pathway

Although our data clearly demonstrate that NOSTRIN induced an alteration of endothelial cell functional transcriptome as well as showing that the anti-angiogenic and anti-inflammatory potential of NOSTRIN is eNOS-independent, the molecular mechanism by which NOSTRIN imparts these functions remained elusive. An analysis of the transcription factor binding sites in the promoters of the NOSTRIN-induced genes in endothelial cells revealed that 13 of the 19 genes had an NFκB response element. We, therefore, sought to investigate both the classical and alternative NFκB activation pathways in all four treatment groups described above. By immunoblot assay, we compared the protein levels of the proteolytically cleaved transcriptionally active forms p50 (NFκB1) and p52 (NFκB2), along with their precursors, p105 and p100. Interestingly, we found a significant ($p < 0.01$) decrease in the p50 subunit in endothelial cells overexpressing NOSTRIN, whereas the corresponding precursor did not change significantly ($p < 0.1$). On the other hand, there was a 16% elevation in p50 protein levels by NOS inhibition alone. Previous reports also suggest that high NO levels lead to inhibition of NFκB activity by several mechanisms (35). There was no significant change in the activation of the alternate NFκB pathway, as shown by the p52 protein levels (Fig. 7, *A* and *B*). We also found that inhibition of NOS by L-NNA had no significant effect on the inhibition of NFκB activation when NOSTRIN levels were high.

To show the specificity of NOSTRIN-mediated down-regulation of NFκB signaling, we stimulated the control and NOSTRIN-overexpressed endothelial cells with TNFα. Within 15 min of TNFα treatment, the p50 levels significantly ($p < 0.005$) increased by 65% in control cells. Interestingly, NOSTRIN significantly ($p < 0.05$) down-regulated p50 levels even in the presence of TNFα (Fig. 7, *C* and *D*). These data clearly indicate that NOSTRIN interferes with the NFκB-signaling pathway by a specific mechanism yet to be determined.

NOSTRIN forms a signaling complex with TNF receptor-associated factor 6 (TRAF6)

NOSTRIN-mediated down-regulation of p50 and the presence of the SH3 domain in NOSTRIN protein led to the hypothesis that NOSTRIN may interact with TRAF6. Proteins containing SH3 domains interact with proline-rich motifs with a P*XX*P consensus sequence flanked by basic residues (36). TRAF-6 contains a putative SH3-interacting sequence: RPTIPR (amino acids 469–474) within the TRAF domain. Besides, TRAF6 is known to inhibit pro-angiogenic signals in endothelial cells (37). In agreement with our hypothesis, TRAF6 was found to co-immunoprecipitate with NOSTRIN, and there was a substantial increase of this complex in NOSTRIN-overexpressing cells as compared with the control (Fig. 7*E*).

NOSTRIN inhibits AKT activation in endothelial cells

TRAF6 is known to be a direct E3 ligase for AKT, which is essential for AKT ubiquitination, membrane recruitment, and phosphorylation upon growth factor stimulation (38). TRAF6 deficiency is known to impair TNF-induced NFκB activation and AKT phosphorylation (39). We, therefore, set out to investigate the functional consequences of NOSTRIN overexpression on AKT phosphorylation in endothelial cells. Our results revealed that there was no major change in expression of AKT in control and NOSTRIN-overexpressing cells, but there was a 46% decrease in the phospho-AKT levels when NOSTRIN was overexpressed (Fig. 7, *F* and *G*). A decline in AKT activation along with abrogation of NFκB signaling in NOSTRIN-overexpressing endothelial cells might be responsible for the change in cellular gene expression leading to the alteration of endothelial cell function.

NOSTRIN-induced down-regulation of NFκB and endothelial cell functional proteins requires SH3 domain and NOSTRIN-TRAF6 interaction

To understand the mechanism of NOSTRIN-mediated down-regulation of endothelial cell functional proteins, three domain deletion constructs of NOSTRIN were made (Fig. 8*A*). Full-length NOSTRIN overexpression, as shown above, significantly ($p < 0.05$) decreased NFκB1 (p50) expression. Interestingly, the deletion of the SH3 domain of NOSTRIN was enough to cause a reversal of NOSTRIN-induced down-regulation of p50. There was no significant ($p < 0.1$) difference in p50 expression between control and NOSTRIN-ΔSH3. The deletion of the ID and HR1 domains along with the SH3 domain did not enhance p50 levels further (Fig. 8, *B* and *C*).

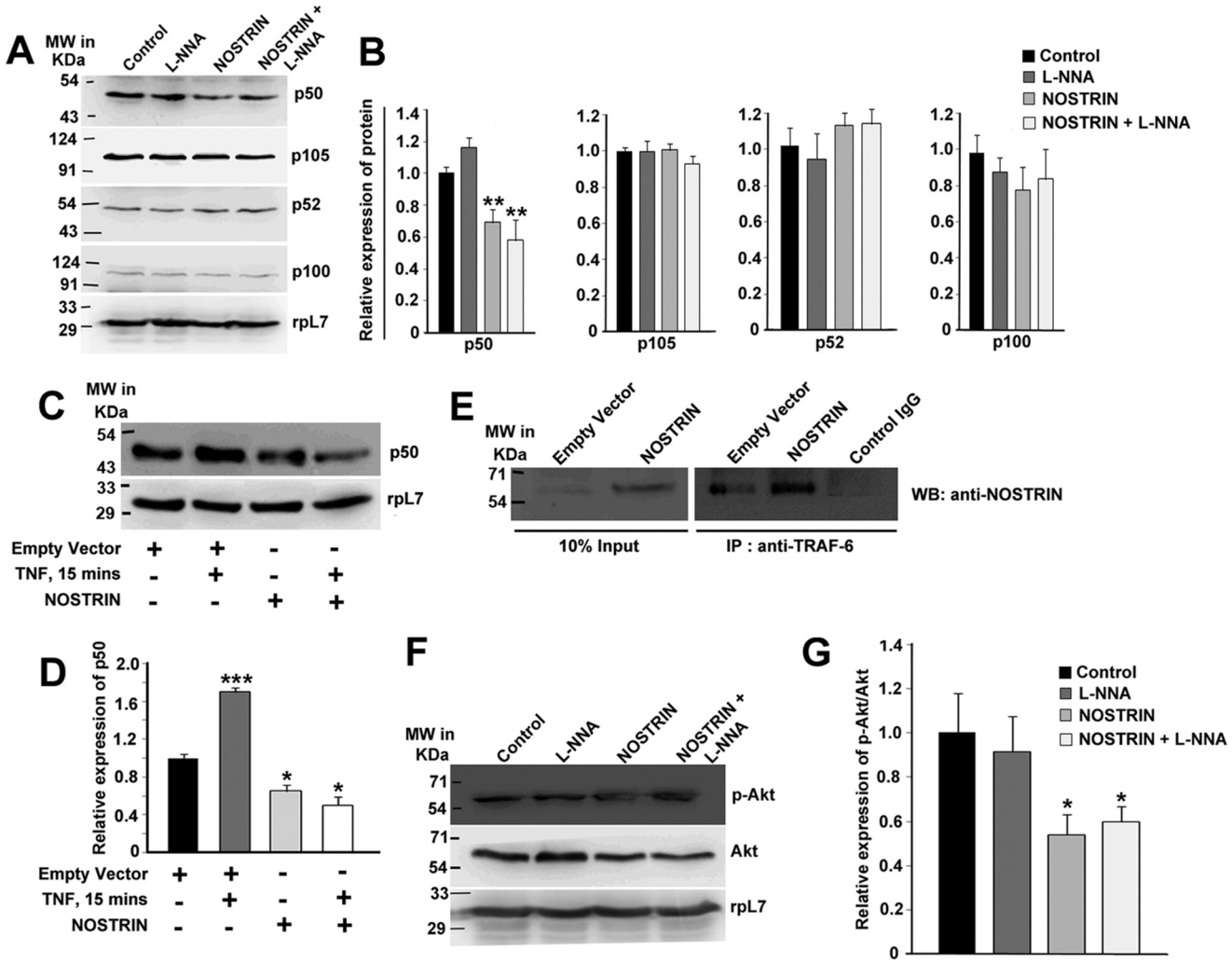

Figure 7. NOSTRIN suppresses NFκB- and AKT-signaling pathway and reverses TNFα-induced NFκB activation by directly interacting with TRAF6. *A*, Western blotting analysis of proteins from endothelial cells of the four treatment groups evaluating the levels of NFκB1 (p105/p50) and NFκB2 (p100/p52). *B*, densitometric quantification of proteins from the Western blotting analysis depicted in *A* normalized to loading control rpL7 using ImageJ software. *Error bars* represent S.E. from three biological replicates. *C*, immunoblot analysis of p50 from endothelial cells in the absence or presence of TNF-α (25 ng/ml) stimulation for 15 min (*lanes 1* and *2*) and of p50 from NOSTRIN-overexpressing endothelial cells in the absence or presence of TNF-α (25 ng/ml) stimulation for 15 min (*lanes 3* and *4*). *D*, quantification of p50 levels from *C* by densitometric analysis normalized to loading control rpL7 using ImageJ software. *Error bars* represent S.E. from three experiments using three different biological samples. *E*, immunoprecipitation with anti-TRAF6 antibody followed by immunoblotting (*WB*) using anti-NOSTRIN antibody in endothelial cells transfected with empty vector or NOSTRIN cDNA. The experiment was repeated three times to ensure reproducibility. *F*, Western blotting analysis of p-AKT and AKT from endothelial cells from the four treatment groups. RpL7 was used as a loading control. *G*, densitometric quantification of p-AKT protein level relative to total AKT protein from three replicates using ImageJ software. *Error bars* represent S.E. from three biological replicates. *, $p < 0.05$; **, $p < 0.01$; and ***, $p < 0.005$.

Furthermore, endothelial cell functional proteins, which were shown to be significantly ($p < 0.05$ or $p < 0.01$) affected by NOSTRIN overexpression, also displayed a partial or complete reversal upon SH3 domain deletion of NOSTRIN, as demonstrated by immunoblot assay (Fig. 8, *D* and *E*). Proteins levels of Flt-1, Mmp2, Plau, Cav1, and Casp3 displayed almost complete recovery upon expression of NOSTRIN-ΔSH3 as compared with full-length NOSTRIN and were not significantly different ($p < 0.5$) as compared with control. Other proteins including Kdr, Tek, Fn1, Itgα5, Itgβ3, and Adam-17 displayed partial recovery on deletion of the SH3 domain of NOSTRIN. Expression of these proteins was significantly higher ($p < 0.05$) in NOSTRIN-ΔSH3 as compared with NOSTRIN but also was significantly ($p < 0.05$) lower as compared with control, indicating the involvement of other regulatory factors for this set of proteins. For all of the functional proteins, deletion of the ID and HR1 domains did not show any further change ($p < 0.1$) as compared with the SH3 domain alone.

It was predicted earlier in our data that NOSTRIN might interact with TRAF6 via its SH3 domain. To directly demonstrate whether NOSTRIN-TRAF6 interaction is mediated by the SH3 domain, immunoprecipitation using TRAF6 antibody followed by Western blotting with NOSTRIN antibody was used. It was found that in cells transfected with NOSTRIN-ΔSH3, the extent of interaction was similar to that of the control, where endogenous NOSTRIN is present, whereas full-length NOSTRIN overexpression significantly increased NOSTRIN-TRAF6 interaction (Fig. 8*F*). To verify the involvement of TRAF6 in NOSTRIN-mediated down-regulation of endothelial cell functional proteins, TRAF6 was overexpressed in the absence or presence of NOSTRIN overexpression in endothelial cells.

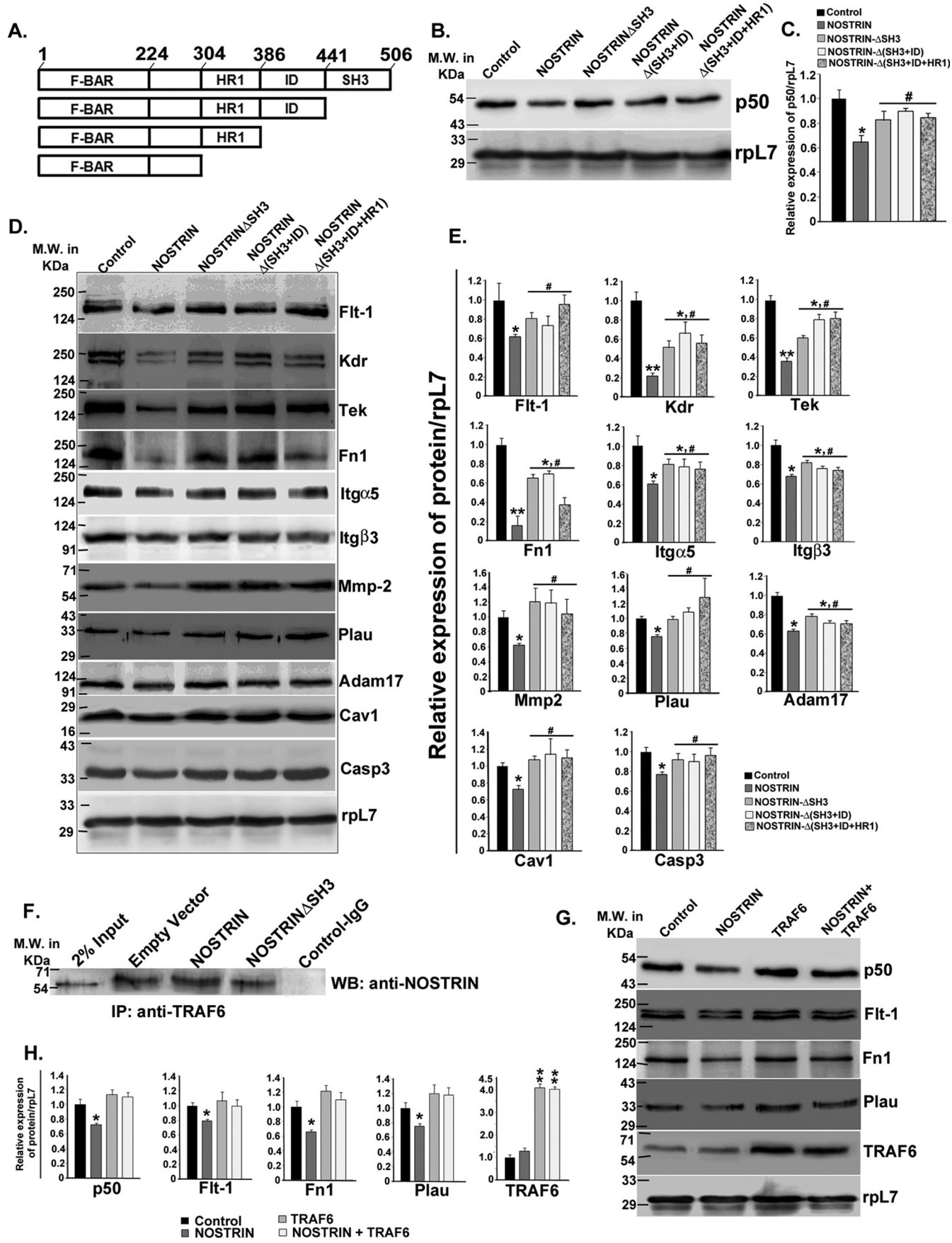
A.
1
224
304
386
441
506
F-BAR
HR1
ID
SH3
B.
M.W. in KDa
Control
NOSTRIN
NOSTRINΔSH3
NOSTRIN Δ(SH3+ID)
NOSTRIN Δ(SH3+ID+HR1)
54
43
33
29
p50
rpL7
C.
Control
NOSTRIN
NOSTRIN-ΔSH3
NOSTRIN-Δ(SH3+ID)
NOSTRIN-Δ(SH3+ID+HR1)
Relative expression of p50/rpL7
D.
M.W. in KDa
Flt-1
Kdr
Tek
Fn1
Itgα5
Itgβ3
Mmp-2
Plau
Adam17
Cav1
Casp3
rpL7
E.
Relative expression of protein/rpL7
Flt-1
Kdr
Tek
Fn1
Itgα5
Itgβ3
Mmp2
Plau
Adam17
Cav1
Casp3
F.
M.W. in KDa
2% Input
Empty Vector
NOSTRIN
NOSTRINΔSH3
Control-IgG
WB: anti-NOSTRIN
IP: anti-TRAF6
G.
M.W. in KDa
Control
NOSTRIN
TRAF6
NOSTRIN+ TRAF6
p50
Flt-1
Fn1
Plau
TRAF6
rpL7
H.
Relative expression of protein/rpL7
p50
Flt-1
Fn1
Plau
TRAF6
Control
NOSTRIN
TRAF6
NOSTRIN + TRAF6

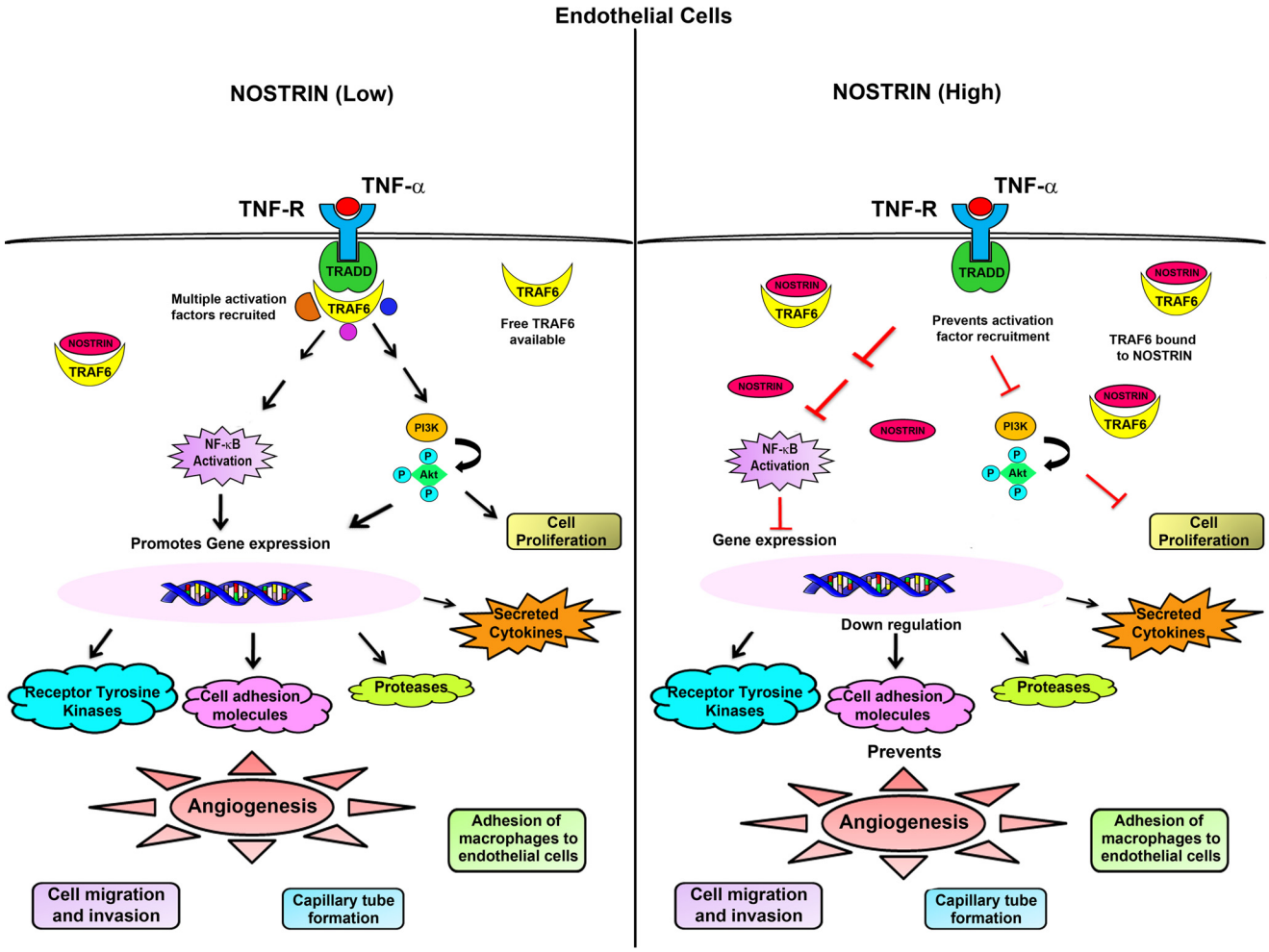

Figure 9. A schematic representation or summary of the alteration in endothelial cell signaling by aberrant NOSTRIN expression. Binding of TNF-α to its cognate receptor leads to the recruitment of several adaptor proteins and activation factors that in turn can activate the NFκB pathway and also promote phosphorylation of AKT. When NOSTRIN levels are low, free TRAF6 molecules are available to bind to TRADD and transduce the signal to downstream activation factors. Rapid activation of the NFκB pathway leads to expression of several pro-angiogenic genes along with production of pro-inflammatory cytokines that are direct targets of the transcription factor NFκB. On the other hand, when NOSTRIN levels are very high, NOSTRIN can bind directly to TRAF6 and thus inhibit its binding to TRADD on TNFα stimulation. This is followed by suppression of NFκB activity along with inhibition of AKT phosphorylation. As a consequence, gene expression is inhibited, and multiple functions of endothelial cells required for angiogenesis are severely compromised.

Expression of p50 and one representative protein from each functional group, as described earlier, was tested in this experiment. In the presence of overexpressed TRAF6, NOSTRIN-induced down-regulation of p50, Flt-1, Fn1, and Plau was completely abrogated (Fig. 8, *G* and *H*).

Taken together, our findings demonstrate that NOSTRIN has a versatile role in endothelial cells. It not only affects the expression of several genes related to invasion and angiogenesis but also pleiotropically regulates several aspects of endothelial cell function including proliferation, invasion, adhesion, and capillary tube formation, primarily by alternating the NFκB pathway, mediated via TRAF6. It may also play a modulatory role in inflammation by regulating the expression of several important chemokines. The overall modulation of endothelial cells by NOSTRIN overexpression is depicted in Fig. 9.

Figure 8. NOSTRIN-mediated effects on endothelial cell functional protein are reversed by deletion of SH3 domain of NOSTRIN, responsible for NOSTRIN-TRAF6 interaction. *A*, domain structure of full-length NOSTRIN and deletion mutants cloned and used for experiments. Amino acid *numbers* are marked at the borders of each domain. *B*, Western blotting analysis using proteins from endothelial cells to evaluate the transcriptionally active form of NFκB1 (p50) in the absence or presence of either full-length NOSTRIN or various deletion mutants of NOSTRIN. *C*, densitometric quantification of p50 from the Western blotting depicted in *B*, normalized to loading control rpL7 using ImageJ software. *Error bars* represent S.E. from three biological replicates. *D*, Western blotting analysis of endothelial cell proteins known to be affected by NOSTRIN in the absence or presence of either full-length or various deletion mutant of NOSTRIN. *E*, quantification of protein levels from those mentioned in *D* by densitometric analysis, normalized to loading control rpL7 using ImageJ software. *Error bars* represent S.E. from three experiments using three different biological samples. *F*, immunoprecipitation (*IP*) with anti-TRAF6 antibody followed by immunoblotting (*WB*) using anti-NOSTRIN antibody in endothelial cells transfected with empty vector, NOSTRIN, or NOSTRINΔSH3 mutant cDNA. The experiment was repeated three times to ensure reproducibility. *G*, Western blotting analysis of p50 and proteins representing three different functional aspect of endothelial cell affected by NOSTRIN in the four treatment groups shows that TRAF6 overexpression overrides the effect of NOSTRIN. *H*, densitometric quantification of proteins from Western blotting depicted in *G*, normalized to loading control rpL7 using ImageJ software. *Error bars* represent S.E. from three biological replicates. *, $p < 0.05$; and **, $p < 0.01$ compared with control; #, $p < 0.05$ compared with full-length NOSTRIN overexpression.

Discussion

In the present study, we have demonstrated a complex network of genes, the expression of which is influenced at both the mRNA and protein levels by ectopic overexpression of NOSTRIN. These genes were broadly annotated as two major endothelial cell functions, *i.e.* angiogenesis and inflammation. The consequence of the changes in gene expression could be extrapolated into NOSTRIN-mediated curtailment of various endothelial cell functional assays, which appears to be mediated by the TRAF6-NFκB signaling axis.

The regulation of angiogenesis is a major aspect in several developmental and pathophysiological processes. It is characterized by a cascade of events tightly regulated by a number of pro- and anti-angiogenic molecules. An intricate balance between the pro- and anti-angiogenic factors governs the complex signaling pathways in endothelial cells. We have demonstrated here that a plethora of pro-angiogenic genes were down-regulated in endothelial cells by aberrant overexpression of NOSTRIN. The initiation of angiogenic signaling occurs primarily by the interaction of pro-angiogenic factors, with their cell surface receptors belonging to the superfamily of tyrosine kinases. Our data revealed that NOSTRIN substantially reduced the expression of receptor tyrosine kinases (RTK). Among them FLT-1/VEGFRI and KDR/VEGFRII function in a similar fashion (40). When bound to VEGF ligands, receptor dimerization and the subsequent activation of cellular signaling cascade leads to angiogenesis. This pathway mediates the majority of its downstream angiogenic effects by microvascular permeability, endothelial cell proliferation, invasion, migration, and the survival of endothelial cells. FLT-1, on the other hand is mainly known to stimulate developmental angiogenesis. PGF, which was also found to be down-regulated by NOSTRIN, is an important ligand for FLT-1. Both the receptors and the ligand, *i.e.* FLT-1 and PGF, were significantly down-regulated by NOSTRIN. These data, therefore, suggest that NOSTRIN might be involved in regulating angiogenesis by fine-tuning the VEGF-signaling pathway.

Other than the VEGF receptors, TIE2/TEK is another class of endothelial specific type-1 trans-membrane protein RTK (41, 42). Loss of TIE2 function results in embryonic death due to failure of the vasculature system to expand (43, 44). TIE2 is required for the maintenance and proliferation of endothelial cells. TEK is activated when bound to ANGIOPOIETIN-1, and TEK signaling is a critical regulator of blood vessel development (45). TEK autophosphorylation promotes endothelial cell migration and survival. NOSTRIN significantly reduced the expression of TEK along with KIT, which is yet another RTK. *Kit* functions as a proto-oncogene, and high levels of KIT expression are associated with several invasive cancers (46, 47). Stem cell factor, a c-KIT ligand, dose-dependently promotes the survival, migration, and capillary tube formation of human umbilical vein endothelial cells (48). To summarize, NOSTRIN is a critical regulator of tyrosine kinase receptors in endothelial cells. Deregulation of RTK activity is one of the major mechanisms by which cancer cells evade cellular restrictions on growth, survival, and migration (49–53). RTKs are well-known clinical targets for the prevention of invasion and angiogenesis in tumors. NOSTRIN-induced down-regulation of RTKs thus might prevent angiogenic signaling in tumor endothelial cells. Our data imply that NOSTRIN may be a potential candidate for the prevention of cancer angiogenesis.

Degradation and remodeling of the basement membrane and the surrounding ECM are followed by the activation and proliferation of endothelial cells during the onset of angiogenesis. Endothelial cells adhere to the ECM during migration and the sprouting of new blood vessels. The survival and proliferation of endothelial cells are promoted by adhesion of cell surface integrins to ECM (54). Our data show that NOSTRIN overexpression led to significant down-regulation of ITGβ3 and ITGα5 along with FN1. FN1 is known to bind to integrin heterodimers ITGα5β1 and ITGαVβ3 (55). Integrins α5 and β3 on endothelial cells potentiate the interaction of endothelial cells with extracellular matrix harboring FN1 (56, 57). A cross-talk between KDR and ITGβ3 is also known to increase adhesion and invasion during vascular development and VEGF-induced angiogenesis (58, 59). The activity of most of the endothelial cell integrins during angiogenesis is regulated primarily at the transcriptional level, and pro-angiogenic factors continuously stimulate integrin expression and activity (60). Furthermore, COL18a1, a component of the extracellular matrix that has structural properties of collagen and proteoglycan and is involved in cell-matrix interactions, was also shown to decrease significantly upon NOSTRIN overexpression (our data). These results suggest that NOSTRIN is a putative inhibitor of endothelial cell adhesion to extracellular matrix. Cell adhesion molecules also play a significant role in cancer progression and metastasis. Both ITGα5 and ITGβ3 are known to potentiate cancer progression and metastasis (61, 62). NOSTRIN-mediated down-regulation of ITGα5 and ITGβ3 therefore indicates that NOSTRIN may inhibit the metastasis of cancer cells.

Other important players in the degradation of extracellular matrix and basement membrane are the proteolytic enzymes. Our data on aberrant NOSTRIN expression leading to down-regulation of PLAU, MMP2, and ADAM-17 have important connotations in this regard. MMP2 levels not only are elevated in all human and animal cancers but also increase remarkably with the developing stages of tumor progression (63). Similarly, ADAM-17 is up-regulated in numerous human cancers (64) and promotes motility, invasion, and sprouting of lymphatic endothelial cells (65). ADAM-17 promotes VEGF-induced angiogenesis *ex vivo* and retinal neovascularization in mice *in vivo* (66, 67). Likewise, PLAU is also positively correlated with tumor neovascularization as well as cancer progression (68, 69). Our data therefore indicate that NOSTRIN may play a significant role in deregulating the expression of proteases important during tumor angiogenesis and cancer progression.

Caveolin-1 is known to regulate vascular tone. Genetic disruption of *Cav*-1 leads to pulmonary hypertension in mice (70). Our data on NOSTRIN-mediated down-regulation of CAV1, therefore, suggest that NOSTRIN may act as an endogenous vasoconstrictor and can induce hypertension. This result revalidates the existing literature of NOSTRIN elevation in pregnancy-induced hypertension and pre-eclampsia (16–18) but cannot support the endothelial cell-specific NOSTRIN-KO mouse data (24). It can therefore be inferred that NOSTRIN,

being an adaptor protein, might have multifaceted functions depending upon the availability of other interacting proteins/stimuli in a particular cell type. Expression of the pro-apoptotic gene *Casp3* was reduced by NOSTRIN overexpression. Because NFκB fundamentally increases cell survival and proliferation, which are reduced on NOSTRIN overexpression, the effect of CASP3 might be masked by this signaling pathway. Further studies are required to gain insights into NOSTRIN-mediated CASP3 down-regulation.

NFκB and AKT-signaling pathways are recognized as positive regulators of cell proliferation and survival as well as promoters of angiogenesis. Constitutively active AKT enhances NFκB activity (71). Several cancers have constitutively activated AKT, and AKT is essential for TNF-α-induced activation of NFκB (72). From various reports it is quite evident that AKT promotes cancer and metastasis in a NFκB-dependent manner. *In vitro* studies showed that drug-resistant cancer cell lines have increased NFκB activity (73). On the other hand, drugs that suppress tumor cell invasion and neovascularization inhibit AKT phosphorylation along with the suppression of NFκB transcriptional activity (74). In sum, AKT and NFκB are regulated coordinately. Our study has demonstrated that NOSTRIN overexpression leads to down-regulation of NFκB signaling along with inhibition of AKT activity. Furthermore, our data on the eNOS-independent NOSTRIN-mediated decrease in endothelial cell proliferation, migration, invasion, adhesion, and VEGF-induced tube formation are the final endorsement of NOSTRIN function in endothelial cells. Thus, NOSTRIN might be a potential endogenous tumor suppressor.

Our data on the direct interaction of NOSTRIN with TRAF6 is intriguing, as this event primarily governs NOSTRIN-induced down-regulation of the NFκB- and AKT-signaling pathways leading to the down-regulation of genes involved in proliferation, invasion, and angiogenesis. Experiments on SH3 domain deletion provides evidence that the NOSTRIN-TRAF6 interaction is mediated by the SH3 domain of NOSTRIN. It was also demonstrated that the SH3 domain is necessary for NOSTRIN-induced down-regulation of p50 as well as other endothelial cell functional proteins. Overexpression of TRAF6 may lead to saturation of TRAF6 binding to available NOSTRIN. Consequently, effects of NOSTRIN that are mediated by binding TRAF6 followed by decline in NFκB pathway is abrogated.

Our data indicate that the SH3 domain of NOSTRIN is involved in the interaction with TRAF6, leading to the anti-angiogenic function of NOSTRIN in endothelial cells. Previous reports show that the SH3 domain of NOSTRIN is also involved in interactions with eNOS (8, 10) leading to its vesicular sequestration. Moreover, it had also been shown that the SH3 domain of NOSTRIN interacts with N-WASP and DYNAMIN, which are involved in cell migration (12). Therefore, the existing literature, as well as our new data, clearly indicates that the function of NOSTRIN is pleiotropic and that the SH3 domain of NOSTRIN is required for NOSTRIN's anti-angiogenic potential. On the other hand, in the presence of FGF-2, the HR1 domain of NOSTRIN interacts with RAC1 and activates its function leading to the angiogenic function of NOSTRIN. Therefore, the function of NOSTRIN is context-specific, and its pro- or anti-angiogenic function is determined by the stimulus that governs the interacting partners.

The NOSTRIN-induced down-regulation of inflammation-related genes such as *IL6* and *Ccl2* in endothelial cells, as shown in our results, is in line with our data on the NOSTRIN-induced decrease in NFκB1 protein. A major aspect of NFκB signaling is its role in inflammation. Gene knockouts of the transcription factors, inhibitors, and kinases in the NFκB signal transduction pathway suggests that activation of the NFκB pathway primarily promotes inflammation (75). Direct induction of the *IL6* gene by NFκB has been shown previously (76, 77). Similarly, the *Ccl2*/*MCP1* promoter can be rapidly induced by NFκB upon activation by LPS or TNF-α (78, 79).

The importance of NOSTRIN under pathophysiological conditions, in particular cancer progression and survival, has been documented in pancreatic ductal adenocarcinoma patients (27, 28). Our data have clearly demonstrated that increased NOSTRIN levels are associated with decreased angiogenic potential as well as diminished expression of angiogenesis and invasion-promoting genes. Hence, our data on the cellular function of NOSTRIN at a molecular level provide the mechanistic explanation as to why elevated levels of NOSTRIN in cancer patients lead to an increased rate of survival. Our data further support this existing clinical report (27, 28) and emphasize the need for screening NOSTRIN in other neoplastic varieties, possibly in view of using it as a potential marker for cancer prognosis.

Although our data completely support the physiological data available for NOSTRIN in human patients, it is not in agreement with the pro-angiogenic function of NOSTRIN in knockout models of mice and zebrafish. NOSTRIN in KO mice have a moderate postnatal pro-angiogenic effect, which could be due to the compensatory overexpression of other F-BAR proteins. Yet another explanation for the different role of NOSTRIN in KO mice and under NOSTRIN-elevated human physiological conditions may be the differential availability and involvement of context-specific NOSTRIN-interacting molecules.

In conclusion, it is inferred from our data that NOSTRIN levels are maintained at a low level in endothelial cells. However, when NOSTRIN is overexpressed due to some pathophysiological conditions (16–18, 20, 27, 28, 19) it may act as an endogenous angiogenesis inhibitor. We predict that the anti-angiogeneic potential of NOSTRIN could be exploited as a novel therapeutic approach to prevent cancer progression and metastasis.

Experimental procedures

Cell culture

Mouse endothelial cell line MS1 and RAW264.7 macrophage cell line were obtained from American Type Culture Collection. Endothelial cells were grown in Dulbecco's modified Eagle's medium, high glucose (Sigma-Aldrich) supplemented with 5% fetal bovine serum (Invitrogen) in the presence of penicillin-streptomycin (Invitrogen) and used at passages 8–15. RAW264.7 macrophage cells were grown in RPMI 1640 (Sigma-Aldrich) supplemented with 10% fetal bovine serum (Invitrogen) in the presence of penicillin-streptomycin (Invit-

rogen) and used at passages 6–10. Cells were maintained in 5% CO_2 at 37 °C in a humidified incubator.

Cloning of mouse NOSTRIN, TRAF6, and mutated NOSTRIN cDNA

Mouse placental RNA was reverse-transcribed using SuperScript III reverse transcriptase (Invitrogen). Full-length mouse NOSTRIN (NM_181547.3) cDNA was amplified from the placental cDNA using LA-TaqDNA polymerase (TaKaRa, Clontech). Primers used for full-length NOSTRIN were: forward, 5′-TATAGGTACCGAT GAGGGACCCACTGACGGA-3′, and reverse, 5′-TAATGCGGCCGCTTATGCCTGTG-TAGCTGTGT-3′. Three deletion mutants of NOSTRIN (ΔSH3, Δ(SH3 + ID), and Δ(SH3 + ID + HR1)) were then amplified from full-length NOSTRIN cDNA. The primers used were: ΔSH3 forward, 5′-TATAGGTACCGATGAGGGAC-CCACTGACGGA-3′, and ΔSH3 reverse, 5′-TAATGCGGC-CGCTTAAT GCTTGCTGGCTTGG-3′; Δ(SH3+ ID) forward, 5′-TATAGGTACCGATGAGGGACCCACTGACGGA-3′, and Δ(SH3+ ID) reverse, 5′-TAATG CGGCCGCTTA GCAG-GTGCTACAGGG-3′; and Δ(SH3+ ID + HR1) forward, 5′-TATAGGTACCGATGAGGGACCCA CTGACGGA-3′, and Δ(SH3+ ID + HR1) reverse, 5′-TAATGCGGCC GCT-TAGGGTTTTAATAAAGACTT-3′. Full-length TRAF6 was also cloned from mouse placental cDNA using the primers: forward, 5′-TATAGGTACCGCGCATGAGTCTCTTA-AACTGTGAGAAC-3′, and reverse, 5′-TAATGCGGCCGC-CTACACCCCCGCATC-3′. All forward primers contained KpnI restriction sites, and reverse primers contained NotI restriction sites. The amplified cDNA were cloned in pCAG-DsRed vector (Addgene) by deleting DsRed.

Transfection and reagents

Transfection was performed using Lipofectamine LTX with Plus reagent (Invitrogen). Based on the experiment, various constructs such as pCAG-NOSTRIN expression vector, pCAG-NOSTRINΔSH3, pCAG-NOSTRINΔ (SH3 + ID), pCAG-NOSTRINΔ (SH3 + ID + HR1), and pCAG-TRAF6 were used. Control cells were transfected with empty vector backbone without DsRed. Transfected cells were incubated for 48 h and subjected to RNA or protein isolation. In each experiment with NOSTRIN overexpression, mRNA levels were assessed by real-time PCR. NOSTRIN expression levels were found to be more or less consistent between replicates as well as between experiments. Cells were also treated with L-NNA (Sigma-Aldrich) at a final concentration of 100 μM for inhibition of NOS. All functional assays were performed at least 24 h after transfection and within 48 h to ensure high levels of NOSTRIN expression.

For siRNA treatment, cells were transfected using Lipofectamine RNAiMAX reagent (Invitrogen). Two prevalidated Silencer Select siRNAs targeting the coding region of NOSTRIN (assay ID: s116394 and s116396, Ambion) were used for down-regulation. Control cells were treated with scrambled siRNA. Cells were treated with siRNAs in a dose-dependent manner, and down-regulations were quantified by real-time PCR. The concentration at which maximum down-regulation occurred was selected for further experiments.

Quantitative real-time PCR analysis

Real-time PCR was done as described elsewhere (80). Briefly, RNA was isolated from cells using TRIzol reagent (Invitrogen) followed by reverse transcription of 5 μg of total RNA using a SuperScript III reverse transcription kit (Invitrogen) according to the manufacturer's instructions. A 10-fold dilution of cDNA and Power SYBR GREEN PCR Master Mix (Applied Biosystems) was used in the PCR reaction. Reactions were run using a 7500 real-time PCR system (Applied Biosystems). Conditions included an initial holding stage at 95 °C for 10 min and then 40 cycles at 95 °C for 15 s and 60 °C for 1 min followed by a dissociation stage of 95 °C for 15 s, 60 °C for 1 min, and then 95 °C for 30 s. At least three different biological replicates were used.

Quantitative RT^2 Profiler PCR array assay

A large-scale quantitative real-time PCR array experiment was performed using a mouse endothelial cell biology RT^2 Profiler PCR array (catalog No. PAMM-015Z, SABiosciences-Qiagen) as per the manufacturer's instruction. The PCR array included 84 SYBR Green-optimized primers related to endothelial cell function that were assessed in a 96-well format. RNA isolated from control and NOSTRIN-overexpressed MS1 cells using TRIzol reagent were further purified using an RNeasy mini kit (Qiagen). The concentration and quality of the RNA were measured using a NanoDrop 2000 Spectrophotometer (ThermoFisher Scientific) followed by fractionation on a formaldehyde gel. The cDNA was synthesized using an RT^2 first strand kit (Qiagen) following genomic DNA elimination, and RT^2 SYBR Green q-PCR Master Mix (Qiagen) was used for the real-time array. Normalization was done using the housekeeping gene, which showed no change in NOSTRIN-overexpressed MS1 cells compared with control. The -fold change in gene expression was calculated by using online software provided by SABiosciences.

MTT cell proliferation assay

An MTT assay (Vybrant® MTT cell proliferation assay kit, Molecular Probes) was performed to monitor the growth rate of endothelial cells. The four treatment groups were as follows: 1) cells transfected with vector backbone (control); 2) cells transfected with vector backbone followed by L-NNA treatment at the end of transfection (L-NNA); 3) cells transfected with NOSTRIN expression vector (NOSTRIN); and 4) cells transfected with NOSTRIN expression vector followed by L-NNA treatment 6 h after transfection (NOSTRIN + L-NNA). Twenty-four hours after transfection the cells were seeded in 96-well plates (5×10^4 cells/well in triplicate for each treatment) and cultured for another 16 h. Ten microliters of 12 mM MTT stock solution in sterile Dulbecco's PBS (DPBS) mixed with 100 μl of Medium 200PRF (Life Technologies) was added to each well. A negative control with similar treatment but without cells was included. The cells were then incubated for 4 h in 5% CO_2 at 37 °C. To each well 100 μl of 10% SDS in 0.01 M HCl was then added, and the color that formed was quantified by a multimode plate reader (PerkinElmer) at 570 nm wavelength after 16 h. Each experiment was repeated a minimum of three times.

BrdU cell proliferation assay

A BrdU cell proliferation assay was performed to revalidate the effect of NOSTRIN on cell proliferation using a kit from Cell Signaling Technology. The four treatments used were similar to that described under "MTT assay." Twenty-four hours after transfection, cells were seeded in 96-well plates in triplicates (1×10^5 cells/well) and cultured for another 24 h in the presence of BrdU solution. The medium was removed, and cells were incubated with a fixing/denaturing solution (100 μl/well) at room temperature for 30 min. The solution was removed, and cells were further incubated with detection antibody (100 μl/well) for 1 h. The wells were washed three times with wash buffer. HRP-conjugated secondary antibody solution (100 μl/well) was added, and cells containing BrdU-bound primary antibody were incubated for 30 min with secondary antibody. Wells were again washed three times followed by the addition of tetramethylbenzidine substrate (TMB, 100 μl/well) and incubated for 15 min. STOP solution was added, and subsequently the absorbance was read at 450 nm wavelength using a multimode plate reader (PerkinElmer).

Nitric oxide assay

NO was measured in the cell supernatants in the form of nitrites using a NO colorimetric assay kit (R&D Systems) according to the manufacturer's protocol. The four treatments used were similar to those described under "MTT assay." Following transfection, cells were cultured in serum-containing medium for 24 h. Then the medium was removed, and the cells were cultured for another 24 h in serum-free Medium 200PRF supplemented with low serum growth supplement (LSGS, Life Technologies). Supernatants were collected, filtered using 10,000 molecular-weight-cutoff filters (catalog No. 431478, Corning) prior to use. The total cell count for each of the wells (three replicates/treatment) was determined by trypsinization after collecting the supernatants. A standard curve was prepared with standard nitrite solutions covering a concentration range of 3.12 to 25 μmol/liter. All samples and standards were allowed to react with Griess reagent I and Griess reagent II (R&D Systems) for 10 min. Absorbance was then read at 540 nm, and nitrite levels were quantified from a four-parameter logistic (4-PL) standard curve (PerkinElmer). The amount of nitrite produced per treatment was then normalized to total number of cells.

Scratch wound assay

The migration ability of endothelial cells was monitored by a scratch wound assay using the four treatment groups as mentioned previously. Twenty-four hours after transfection a confluent monolayer was observed. Cells were then treated with mitomycin C for 2 h to inhibit cell proliferation and washed extensively. The medium was removed, and cells were wounded by scraping with disposable cell combs (cell comb scratch assay kit, catalog No. 17-10191, Merck Millipore). A "cell-free" area with a width of ~700 μm was created. Cells were immediately washed with DPBS to remove any detached cells from the wound area. Phase contrast images were captured in multiple fields immediately after scratching the cell monolayer ($t = 0$), and every 6 h until 24 h post-wounding ($t = 24$) using a Leica microscope. Cells are returned to 37 °C, 5% CO_2 between imaging sessions. The length of the wound filled by the migrating cells were measured using Leica Application Suite X (LAS X) software (Leica Microsystems). The percentage of wound closure was calculated based on the equation $((L_i - L_t)/L_i) \times 100\%$, where L_i is the length of wound at $t = 0$ h and L_t is the length of wound following t hours of culture.

Cell invasion assay

Cellular invasive activities *ex vivo* were measured using a two-chambered cell invasion assay kit (ECM550, Chemicon, Merck Millipore). Endothelial cells belonging to the four treatment groups as described under "MTT assay" were cultured for 24 h following transfection. Cells were then trypsinized and seeded onto ECMatrix^{TM} containing Transwell inserts (1.5×10^5 cells/insert) in serum-free medium. Triplicates were used for each of the four treatments. 10% FBS-containing medium was added to the lower chamber. Cells were then allowed to migrate for 24 h in 5% CO_2 at 37 °C. The non-invaded cells were then removed from the interior of the inserts using cotton-tipped swabs. Migrated cells attached to the lower surface of the membrane were stained with the staining solution provided in the kit for 30 min. Cells were visualized using a Leica microscope and counted. The invaded cells were also quantified by dissolving the stained cells at the lower surface of the membrane with 10% acetic acid and measuring the absorbance at 560 nm.

Endothelial tube formation assay

Low passage (P5–P7) endothelial cells were thawed and grown in serum-free and antibiotic-free Medium 200 (Life Technologies) supplemented with low serum growth supplement (Life Technologies). Endothelial cells of the four treatment groups described above were cultured for 24 h following transfection. Three-dimensional basement membrane matrix (catalog No. 356234, BD Biosciences) gels were prepared in 96-well tissue culture dishes (50 μl/well). Cells were then trypsinized with 0.05% trypsin and plated on basement membrane matrix-coated wells (20,000 cells/well) in the presence of 50 ng/ml VEGF (R&D Systems). After 12 h, the tubes were examined microscopically and photographed. Quantification was done based on observable number of tubes, number of branch points, and number of loops, using Wimasis image analysis software.

Cell adhesion assay

Adhesion of macrophage cells to endothelial cells of the four treatment groups mentioned previously was assessed using a Vybrant cell adhesion assay kit (Molecular Probes, catalog No.V-13181). Twenty-four hours after transfection, the cells were trypsinized, counted, and seeded in equal numbers (80,000/well) onto two different 96-well black polystyrene microplates with transparent bottoms (catalog No. 353219, BD Falcon) and grown for another 24 h. Each treatment had triplicates of cells per plate. RAW264.7 macrophage cells were labeled with 5 μM calcein AM (Molecular Probes) for 45 min at 37 °C, washed with RPMI medium, resuspended, and plated over confluent monolayers of endothelial cells in one of the two

96-well plates used (Plate 1). Cells of the other plate (Plate 2) were trypsinized, and the total cell count for each of the wells was determined. Calcein-labeled macrophages were allowed to adhere to endothelial cells plated in Plate 1 for 2 h at 37°C with 5% CO_2. Non-adherent cells were removed by washing with prewarmed RPMI medium. Adhesion of macrophages to endothelial cells was visualized using a Leica microscope. The adhered, labeled cells were then lysed with 0.1% Triton X-100 in 50 mM Tris-HCl buffer, and adhesion was quantified by measuring the fluorescence relative to total number of endothelial cells.

Western blotting analysis

Western blotting was performed as described previously (81). Briefly, endothelial cells from the four treatment groups were lysed in radioimmune precipitation assay buffer (20 mM Tris-HCl, pH 7.5, 150 mM NaCl, 1 mM Na_2EDTA, 1 mM EGTA, 1% Nonidet P-40, 1% sodium deoxycholate, 2.5 mM sodium pyrophosphate, 1 mM β-glycerophosphate, 0.2 mM PMSF, and 1 mM sodium orthovanadate) supplemented with protease inhibitor mixture (Sigma-Aldrich). The cell lysates were fractionated by SDS-PAGE (Bio-Rad) and transferred onto nitrocellulose membrane. An ECL reagent, Luminata Forte (Millipore) was used for chemiluminescence signal detection. Images were acquired using the ChemiDoc imaging system (UVP, LLC, Upland, CA), and band intensities were quantified with ImageJ software.

Immunoprecipitation

Endothelial cell lysates prepared in radioimmune precipitation assay buffer supplemented with protease inhibitor mixture (Sigma-Aldrich) were prepared as described above. The concentration of protein was estimated using Bradford reagent from Bio-Rad. Cell lysates from various treatments were incubated overnight with either control isotype-matched IgG or TRAF6 antibody (BioLegend, catalog No. 654502) at 4 °C to allow for the formation of the antigen-antibody complex. PureProteome protein A/G mix-magnetic beads (Millipore) were used to capture this complex and eluted under denaturing conditions using SDS-PAGE loading buffer as per the manufacturer's protocol.

Antibodies

Anti-NOSTRIN (ab116374) antibody was purchased from Abcam and was used in 1:100 dilutions. Other primary antibodies were purchased from either Cell Signaling Technology and used in 1:1000 dilutions or from Santa Cruz Biotechnology and used in 1:250 dilutions. Antibodies obtained from Cell Signaling Technology are as follows: anti-caspase-3 (catalog No. 9665), anti-caveolin-1 (catalog No. 3267), anti-integrin α5 (catalog No. 4705), anti-integrin β3 (catalog No. 13166), anti-VEGF receptor-2/KDR (catalog No. 2472), anti-c-KIT (catalog No. 3074), anti-eNOS (catalog No. 9572), anti-phospho-eNOS (catalog No. 9571), anti-AKT (catalog No. 4691), anti-phospho-AKT (catalog No. 4060), anti-NFκB1 p105/p50 (catalog No. 12540), and anti-NFκB2 p100/p52 (catalog No. 4882). Those procured from Santa Cruz Biotechnology were: anti-TACE/ADAM-17 (sc-6416), anti-COL18A1 (sc-16651), anti-Flt-1 (sc-316), anti-fibronectin (sc-6952), anti-MMP-2 (sc-10736), anti-PlGF (sc-1883), anti-uPA (sc-14019), and anti-TIE-2/TEK (sc-324). HRP-conjugated goat anti-rabbit antibodies were purchased from Cell Signaling Technology, and HRP-conjugated donkey anti-goat antibodies were purchased from Santa Cruz Biotechnology. Both of the secondary antibodies were used in 1:2000 dilutions.

Enzyme-linked immunosorbent assay

Cells were plated in a 35-mm dish for transient transfection, either with vector backbone or *Nostrin* cDNA, and kept for 24 h to allow overexpression of NOSTRIN. Then the medium was replaced with serum-free M200-PRF Medium, and cells were cultured for another 24 h. Serum-free conditioned medium was then collected and subsequently analyzed by mouse-specific ELISA kits. Expression of IL6, CCL2, and CCL5 was determined using a mouse IL-6 ELISA MAX™ Deluxe kit, a mouse MCP-1 (CCL2) ELISA MAX™ Deluxe kit (BioLegend), and a RANTES ELISA kit (Thermo Scientific), respectively, as per the manufacturers' instruction.

Statistical analysis

All data were analyzed by Student's *t* test for comparison of independent means, using at least three biological replicates. For all experiments performed, $p < 0.05$ was considered significant.

Author contributions—S. C. and R. A. designed and planned the experiments, and S. C. performed the experiments. S. C. and R. A. analyzed the results, wrote the manuscript, and approved the final version.

Acknowledgments—We thank Priyanka Sengupta and Safirul Islam for assisting in the wound healing assay.

References

1. Yoo, S. Y., and Kwon, S. M. (2013) Angiogenesis and its therapeutic opportunities. *Mediators Inflamm.* **2013,** 127170
2. Carmeliet, P. (2003) Angiogenesis in health and disease. *Nat. Med.* **9,** 653–660
3. Chakraborty, S., and Ain, R. (2016) Endothelial cell biology: assessment of endothelial cell function, in *Trends in Experimental Biology*, pp. 1–21, Excel India Publishers, New Delhi, India
4. Adams, R. H., and Alitalo, K. (2007) Molecular regulation of angiogenesis and lymph-angiogenesis. *Nat. Rev. Mol. Cell Biol.* **8,** 464–478
5. De Caterina, R., Libby, P., Peng, H. B., Thannickal, V. J., Rajavashisth, T. B., Gimbrone, M. A.. Jr., Shin, W. S., and Liao, J. K. (1995) Nitric oxide decreases cytokine-induced endothelial activation. Nitric oxide selectively reduces endothelial expression of adhesion molecules and proinflammatory cytokines. *J. Clin. Invest.* **96,** 60–68
6. Ignarro, L. J., Cirino, G., Casini, A., and Napoli, C. (1999) Nitric oxide as a signaling molecule in the vascular system: an overview. *J. Cardiovasc. Pharmacol.* **34,** 879–886
7. Kruzliak, P., Kovacova, G., and Pechanova, O. (2013) Therapeutic potential of nitric oxide donors in the prevention and treatment of angiogenesis-inhibitor-induced-hypertension. *Angiogenesis* **16,** 289–295
8. Zimmermann, K., Opitz, N., Dedio, J., Renne, C., Muller-Esterl, W., and Oess, S. (2002) NOSTRIN: a protein modulating nitric oxide release and subcellular distribution of endothelial nitric oxide synthase. *Proc. Natl. Acad. Sci. U.S.A.* **99,** 17167–17172
9. Choi, Y. J., Cho, S. Y., Kim, H. W., Kim, J. A., Bae, S. H., and Park, S. S. (2005) Cloning and characterization of mouse disabled 2 interacting pro-

tein 2, a mouse orthologue of human NOSTRIN. *Biochem. Biophys. Res. Commun.,* **326,** 594–599
10. Schilling, K., Opitz, N., Wiesenthal, A., Oess, S., Tikkanen, R., Müller-Esterl, W., and Icking, A. (2006) Translocation of endothelial nitric-oxide synthase involves a ternary complex with caveolin-1 and NOSTRIN. *Mol. Cell. Biol.* **17,** 3870–3880
11. Xu, X. Y., Pang, W. J., Wen, Z. N., and Xiang, W. P. (2013) Changes in human umbilical vein endothelial cells induced by endothelial nitric oxide synthase traffic inducer. *J. Huazhong Univ. Sci. Technolog. Med. Sci.* **33,** 272–276
12. Icking, A., Matt, S., Opitz, N., Wiesenthal, A., Müller-Esterl, W., and Schilling, K. (2005) NOSTRIN functions as a homotrimeric adaptor protein facilitating internalization of eNOS. *J. Cell Sci.* **118,** 5059–5069
13. Icking, A., Schilling, K., Wiesenthal, A., Opitz, N., and Müller-Esterl, W. (2006) FCH/Cdc15 domain determines distinct subcellular localization of NOSTRIN. *FEBS Lett.* **580,** 223–228
14. Mukhopadhyay, S., Xu, F., and Sehgal, P. B. (2007) Abberant cytoplasmic sequestration of eNOS in endothelial cells after monocrotaline, hypoxia, and senescence: live-cell caveolar and cytoplasmic NO imaging. *Am. J. Physiol. Heart Circ. Physiol.* **292,** H1373–H1389
15. McCormick, M. E., Goel, R., Fulton, D., Oess, S., Newman, D., and Tzima, E. (2011) Platelet-endothelial cell adhesion molecule-1 regulates endothelial NO synthase activity and localization through signal transducers and activators of transcription 3-dependent NOSTRIN expression. *Arterioscler. Thromb. Vasc. Biol.* **31,** 643–649
16. Xiang, W., Chen, H., Xu, X., Zhang, M., and Jiang, R. (2005) Expression of endothelial nitric oxide synthase traffic inducer in the placentas of women with pre-eclampsia. *Int. J. Gynaecol. Obstet.* **89,** 103–107
17. Xiang, W., Chen, H., Guo, Y., and Shen, H. (2006) Expression of endothelial nitric oxide synthase traffic inducer in the placenta of pregnancy induced hypertension. *J. Huazhong Univ. Sci. Technolog. Med. Sci.* **26,** 356–358
18. Xiang, W., Chen, H., Hu, L., and Xu, X. (2009) Endothelial nitric oxide synthase traffic inducer in the umbilical vessels of the patients with preeclampsia. *J. Huazhong Univ. Sci. Technolog Med. Sci.* **29,** 243–245
19. Xiang, W. P., Wen, Z. N., Hu, L., Li, H. G., and Xiong, C. L. (2011) Expression of NOSTRIN in the testis tissue of azoospermia patients. *Zhonghua Nan Ke Xue* **17,** 38–42
20. Mookerjee, R. P., Wiesenthal, A., Icking, A., Hodges, S. J., Davies, N. A., Schilling, K., Sen, S., Williams, R., Novelli, M., Müller-Esterl, W., and Jalan, R. (2007) Increased gene and protein expression of the novel eNOS regulatory protein NOSTRIN and a variant in alcoholic hepatitis. *Gastroenterology* **132,** 2533–2541
21. Wiesenthal, A., Hoffmeister, M., Siddique, M., Kovacevic, I., Oess, S., Müller-Esterl, W., and Siehoff-Icking, A. (2009) NOSTRINβ: a shortened NOSTRIN variant with a role in transcriptional regulation. *Traffic* **10,** 26–34
22. Kim, H. W., Choi, Y. J., Kim, J. A., Bae, S. H., Kim, K. R., and Park, S. S. (2005) Mouse disabled 2-interacting protein 2 functions as a transcriptional repressor through direct binding onto its own promoter. *Biochem. Biophys. Res. Commun.* **337,** 75–81
23. Bae, S. H., Choi, Y. J., Kim, K. H., and Park, S. S. (2014) Identification of the cis-element and bZIP DNA binding motifs for the autogenous negative control of mouse NOSTRIN. *Biochem. Biophys. Res. Commun.* **443,** 924–931
24. Kovacevic, I., Hu, J., Siehoff-Icking, A., Opitz, N., Griffin, A., Perkins, A. C., Munn, A. L., Müller-Esterl, W., Popp, R., Fleming, I., Jungblut, B., Hoffmeister, M., and Oess, S. (2012) The F-BAR protein NOSTRIN participates in FGF signal transduction and vascular development. *EMBO J.* **31,** 3309–3322
25. Kirsch, T., Kaufeld, J., Korstanje, R., Hentschel, D. M., Staggs, L., Bollig, F., Beese, M., Schroder, P., Boehme, L., Haller, H., and Schiffer, M. (2013) Knockdown of the hypertension-associated gene NOSTRIN alters glomerular barrier function in zebrafish (*Danio rerio*). *Hypertension* **62,** 726–730
26. Zobel, T., Brinkmann, K., Koch, N., Schneider, K., Seemann, E., Fleige, A., Qualmann, B., Kessels, M. M., and Bogdan, S. (2015) Cooperative functions of the two F-BAR proteins Cip4 and Nostrin in the regulation of E-cadherin in epithelial morphogenesis. *J. Cell Sci.* **128,** 1453
27. Haider, S., Wang, J., Nagano, A., Desai, A., Arumugam, P., Dumartin, L., Fitzgibbon, J., Hagemann, T., Marshall, J. F., Kocher, H. M., Crnogorac-Jurcevic, T., Scarpa, A., Lemoine, N. R., and Chelala, C. (2014) A multigene signature predicts outcome in patients with pancreatic ductal adenocarcinoma. *Genome Med.* **6,** 105–125
28. Wang, J., Yang, S., He, P., Schetter, A. J., Gaedcke, J., Ghadimi, B. M., Ried, T., Yfantis, H. G., Lee, D. H., Gaida, M. M., Hanna, N., Alexander, H. R., and Hussain, S. P. (2016) Endothelial nitric oxide synthase traffic inducer (NOSTRIN) is a negative regulator of disease aggressiveness in pancreatic cancer. *Clin. Cancer Res.* **22,** 5992–6001
29. Taylor, K. L., Oates, R. K., Grane, R., Leaman, D. W., Borden, E. C., and Lindner, D. J. (2006) IFN-α1,8 inhibits tumor-induced angiogenesis in murine angiosarcomas. *J. Interferon Cytokine Res.* **26,** 353–361
30. Arbiser, J. L., Larsson, H., Claesson-Welsh, L., Bai, X., LaMontagne, K., Weiss, S. W., Soker, S., Flynn, E., and Brown, L. F. (2000) Overexpression of VEGF 121 in immortalized endothelial cells causes conversion to slowly growing angiosarcoma and high level expression of the VEGF receptors VEGFR-1 and VEGFR-2 *in vivo*. *Am. J. Pathol.* **156,** 1469–1476
31. Hasenstein, J. R., Kasmerchak, L., Buehler, D., Hafez, G. R., Cleary, K., Moody, J. S., and Kozak, K. R. (2012) Efficacy of Tie2 receptor antagonism in angiosarcoma. *Neoplasia* **14,** 131–140
32. Li, X. D., Cheng, Y. T., Yang, Y. J., Meng, X. M., Zhao, J. L., Zhang, H. T., Wu, Y. J., You, S. J., and Wu, Y. L. (2012) PKA mediated eNOS phosphorylation in the protection of ischemic preconditioning against no reflow. *Microvasc. Res.* **84,** 44–54
33. Rossoni, L. V., Wareing, M., Wenceslau, C. F., Al-Abri, M., Cobb, C., and Austin, C. (2011) Acute simvastatin increases endothelial nitric oxide synthase phosphorylation via AMP-activated protein kinase and reduces contractility of isolated rat mesenteric resistance arteries. *Clin. Sci.* (*Lond.*) **121,** 449–458
34. Napoli, C., Paolisso, G., Casamassimi, A., Al-Omran, M., Barbieri, M., Sommese, L., Infante, T., and Ignarro, L. J. (2013) Effects of nitric oxide on cell proliferation: novel insights. *J. Am. Coll. Cardiol.* **62,** 89–95
35. Bonavida, B., Baritaki, S., Huerta-Yepez, S., Vega, M., Jazirehi, A., and Berenson, J. (2010) Nitric oxide donors are a new class of anti-cancer therapeutics, in *Nitric Oxide (NO) and Cancer: Prognosis, Prevention, and Therapy*, pp. 458–462, Humana Press, New York, NY
36. Brown, M. T., and Cooper, J. A. (1996) Regulation, substrates and functions of src. *Biochim. Biophys. Acta* **1287,** 121–149
37. Bruneau, S., Datta, D., Flaxenburg, J. A., Pal, S., and Briscoe, D. M. (2012) TRAF6 inhibits proangiogenic signals in endothelial cells and regulates the expression of vascular endothelial growth factor. *Biochem. Biophys. Res. Commun.* **419,** 66–71
38. Yang, W. L., Zhang, X., and Lin, H. K. (2010) Emerging role of Lys-63 ubiquitination in protein kinase and phosphatase activation and cancer development. *Oncogene* **29,** 4493–4503
39. Yoon, K., Jung, E. J., Lee, S. R., Kim, J., Choi, Y., and Lee, S. Y. (2008) TRAF6 deficiency promotes TNF-induced cell death through inactivation of GSK3β. *Cell Death Differ.* **15,** 730–738
40. Kanno, S., Oda, N., Abe, M., Terai, Y., Ito, M., Shitara, K., Tabayashi, K., Shibuya, M., and Sato, Y. (2000) Roles of two VEGF receptors, Flt-1 and KDR, in the signal transduction of VEGF effects in human vascular endothelial cells. *Oncogene* **19,** 2138–2146
41. Ward, N. L., and Dumont, D. J. (2002) The angiopoietins and Tie2/Tek: adding to the complexity of cardiovascular development. *Semin. Cell Dev. Biol.* **13,** 19–27
42. Yancopoulos, G. D., Davis, S., Gale, N. W., Rudge, J. S., Wiegand, S. J., and Holash, J. (2000) Vascular-specific growth factors and blood vessel formation. *Nature* **407,** 242–248
43. Dumont, D. J., Gradwohl, G., Fong, G. H., Puri, M. C., Gertsenstein, M., Auerbach, A., and Breitman, M. L. (1994) Dominant-negative and targeted null mutations in the endothelial receptor tyrosine kinase, tek, reveal a critical role in vasculogenesis of the embryo. *Genes Dev.* **8,** 1897–1909
44. Sato, T. N., Tozawa, Y., Deutsch, U., Wolburg-Buchholz, K., Fujiwara, Y., Gendron-Maguire, M., Gridley, T., Wolburg, H., Risau, W., and Qin, Y.

(1995) Distinct roles of the receptor tyrosine kinases Tie-1 and Tie-2 in blood vessel formation. *Nature* **376,** 70–74
45. Jeansson, M., Gawlik, A., Anderson, G., Li, C., Kerjaschki, D., Henkelman, M., and Quaggin, S. E. (2011) Angiopoietin-1 is essential in mouse vasculature during development and in response to injury. *J. Clin. Invest.* **121,** 2278–2289
46. Eroğlu, A., and Sari, A. (2007) Expression of c-kit proto-oncogene product in breast cancer tissues. *Med. Oncol.* **24,** 169–174
47. Rocha-Zavaleta, L., Huitron, C., Cacéres-Cortés, J. R., Alvarado-Moreno, J. A., Valle-Mendiola, A., Soto-Cruz, I., Weiss-Steider, B., and Rangel-Corona, R. (2004) Interleukin-2 (IL-2) receptor-$\beta\gamma$ signaling is activated by c-Kit in the absence of IL-2 or by exogenous IL-2 via JAK3/STAT5 in human papillomavirus-associated cervical cancer. *Cell. Signal.* **16,** 1239–1247
48. Matsui, J., Wakabayashi, T., Asada, M., Yoshimatsu, K., and Okada, M. (2004) Stem cell factor/*c*-kit signaling promotes the survival, migration, and capillary tube formation of human umbilical vein endothelial cells. *J. Biol. Chem.* **279,** 18600–18607
49. Millauer, B., Shawver, L. K., Plate, K. H., Risau, W., and Ullrich, A. (1994) Glioblastoma growth inhibited *in vivo* by a dominant-negative Flk-1 mutant. *Nature* **367,** 576–579
50. Millauer, B., Longhi, M. P., Plate, K. H., Shawver, L. K., Risau, W., Ullrich, A., and Strawn, L. M. (1996) Dominant-negative inhibition of Flk-1 suppresses the growth of many tumor types *in vivo*. *Cancer Res.* **56,** 1615–1620
51. Fong, T. A., Shawver, L. K., Sun, L., Tang, C., App, H., Powell, T. J., Kim, Y. H., Schreck, R., Wang, X., Risau, W., Ullrich, A., Hirth, K. P., and McMahon, G. (1999) SU5416 is a potent and selective inhibitor of the vascular endothelial growth factor receptor (Flk-1/KDR) that inhibits tyrosine kinase catalysis, tumor vascularization, and growth of multiple tumor types. *Cancer Res.* **59,** 99–106
52. Shaheen, R. M., Davis, D. W., Liu, W., Zebrowski, B. K., Wilson, M. R., Bucana, C. D., McConkey, D. J., McMahon, G., and Ellis, L. M. (1999) Antiangiogenic therapy targeting the tyrosine kinase receptor for vascular endothelial growth factor receptor inhibits the growth of colon cancer liver metastasis and induces tumor and endothelial cell apoptosis. *Cancer Res.* **59,** 5412–5416
53. Casaletto, J. B., and McClatchey, A. I. (2012) Spatial regulation of receptor tyrosine kinases in development and cancer. *Nat. Rev. Cancer* **12,** 387–400
54. Giancotti, F. G., and Ruoslahti, E. (1999) Integrin signaling. *Science* **285,** 1028–1032
55. Danen, E. H., Sonneveld, P., Brakebusch, C., Fassler, R., and Sonnenberg, A. (2002) The fibronectin-binding integrins $\alpha5\beta1$ and $\alpha v\beta3$ differentially modulate RhoA-GTP loading, organization of cell matrix adhesions, and fibronectin fibrillogenesis. *J. Cell Biol.* **159,** 1071–1086
56. Morgan, M. R., Humphries, M. J., and Bass, M. D. (2007) Synergistic control of cell adhesion by integrins and syndecans. *Nat. Rev. Mol. Cell Biol.* **8,** 957–969
57. Desgrosellier, J. S., and Cheresh, D. A. (2010) Integrins in cancer: biological implications and therapeutic opportunities. *Nat. Rev. Cancer* **10,** 9–22
58. Somanath, P. R., and Malinin, N. L., and Byzova, T. V. (2009) Cooperation between integrin $\alpha\beta3$ and VEGFR2 in angiogenesis. *Angiogenesis* **12,** 177–185
59. Mahabeleshwar, G. H., Feng, W., Reddy, K., Plow, E. F., and Byzova, T. V. (2007) Mechanisms of integrin-vascular endothelial growth factor receptor cross-activation in angiogenesis. *Circ. Res.* **101,** 570–580
60. Avraamides, C. J., Garmy-Susini, B., and Varner, J. A. (2008) Integrins in angiogenesis and lymphangiogenesis. *Nat. Rev. Cancer* **8,** 604–617
61. Bhaskar, V., Zhang, D., Fox, M., Seto, P., Wong, M. H., Wales, P. E., Powers, D., Chao, D. T., Dubridge, R. B., and Ramakrishnan, V. (2007) A function blocking anti-mouse integrin $\alpha5\beta1$ antibody inhibits angiogenesis and impedes tumor growth *in vivo*. *J. Transl. Med.* **5,** 61–71
62. Robinson, S. D., Reynolds, L. E., Kostourou, V., Reynolds, A. R., da Silva, R. G., Tavora, B., Baker, M., Marshall, J. F., and Hodivala-Dilke, K. M. (2009) $\alpha v\ \beta3$ integrin limits the contribution of neuropilin-1 to vascular endothelial growth factor-induced angiogenesis. *J. Biol. Chem.* **284,** 33966–33981
63. Coussens, L. M., Fingleton, B., and Matrisian, L. M. (2002) Matrix metalloproteinase inhibitors and cancer: trials and tribulations. *Science* **295,** 2387–2392
64. Murphy, G. (2008) The ADAMs: signaling scissors in the tumor microenvironment. *Nat. Rev. Cancer* **8,** 929–941
65. Mezyk-Kopeć, R., Wyroba, B., Stalińska, K., Próchnicki, T., Wiatrowska, K., Kilarski, W. W., Swartz, M. A., and Bereta, J. (2015) ADAM17 promotes motility, invasion, and sprouting of lymphatic endothelial cells. *PLoS One* **10,** e0132661
66. Chikaraishi, Y., Shimazawa, M., Yokota, K., Yoshino, K., and Hara, H. (2009) CB-12181, a new azasugar-based matrix metalloproteinase/tumor necrosis factor-α converting enzyme inhibitor, inhibits vascular endothelial growth factor-induced angiogenesis *in vitro* and retinal neovascularization *in vivo*. *Curr. Neurovasc. Res.* **6,** 140–147
67. Göoz, P., Göoz, M., Baldys, A., and Hoffman, S. (2009) ADAM-17 regulates endothelial cell morphology, proliferation, and *in vitro* angiogenesis. *Biochem. Biophys. Res. Commun.* **380,** 33–38
68. Hildenbrand, R., Dilger, I., Hörlin, A., and Stutte, H. J. (1995) Urokinase plasminogen activator induces angiogenesis and tumor vessel invasion in breast cancer. *Pathol. Res. Pract.* **191,** 403–409
69. Kaneko, T., Konno, H., Baba, M., Tanaka, T., and Nakamura, S. (2003) Urokinase-type plasminogen activator expression correlates with tumor angiogenesis and poor outcome in gastric cancer. *Cancer Sci.* **94,** 43–49
70. Le Lay, S., and Kurzchalia, T. V. (2005) Getting rid of caveolins: phenotypes of caveolin-deficient animals. *Biochim. Biophys. Acta* **1746,** 322–333
71. Bai, D., Ueno, L., and Vogt, P. K. (2009) Akt-mediated regulation of NFκB and the essentialness of NFκB for the oncogenicity of PI3K and Akt. *Int. J. Cancer* **125,** 2863–2870
72. Ozes, O. N., Mayo, L. D., Gustin, J. A., Pfeffer, S. R., Pfeffer, L. M., and Donner, D. B. (1999) NF-κB activation by tumour necrosis factor requires the Akt serine-threonine kinase. *Nature* **401,** 82–85
73. Arlt, A., Gehrz, A., Müerköster, S., Vorndamm, J., Kruse, M. L., Fölsch, U. R., and Schäfer, H. (2003) Role of NF-κB and Akt/PI3K in the resistance of pancreatic carcinoma cell lines against gemcitabine-induced cell death. *Oncogene* **22,** 3243–3251
74. Nakabayashi, H., and Shimizu, K. (2012) Involvement of Akt/NF-κB pathway in antitumor effects of parthenolide on glioblastoma cells *in vitro* and *in vivo*. *BMC Cancer* **12,** 453
75. Lawrence, T. (2009) The nuclear factor NF-κB pathway in inflammation. *Cold Spring Harb. Perspect. Biol.* **1,** a001651
76. Libermann, T. A., and Baltimore, D. (1990) Activation of interleukin-6 gene expression through the NF-κB transcription factor. *Mol. Cell. Biol.* **10,** 2327–2334
77. Son, Y. H., Jeong, Y. T., Lee, K. A., Choi, K. H., Kim, S. M., Rhim, B. Y., and Kim, K. (2008) Roles of MAPK and NF-κB in interleukin-6 induction by lipopolysaccharide in vascular smooth muscle cells. *J. Cardiovasc. Pharmacol.* **51,** 71–77
78. Ueda, A., Ishigatsubo, Y., Okubo, T., and Yoshimura, T. (1997) Transcriptional regulation of the human monocyte chemoattractant protein-1 gene: cooperation of two NF-κB sites and NF-κB/Rel subunit specificity. *J. Biol. Chem.* **272,** 31092–31099
79. Teferedegne, B., Green, M. R., Guo, Z., and Boss, J. M. (2006) Mechanism of action of a distal NF-κB-dependent enhancer. *Mol. Cell. Biol.* **26,** 5759–5770
80. Saha, S., Choudhury, J., and Ain, R. (2015) MicroRNA-141–3p and miR-200a-3p regulate insulin-like growth factor 2 during mouse placental development. *Mol. Cell. Endocrinol.* **414,** 186–193
81. Ain, R., Dai, G., Dunmore, J. H., Godwin, A. R., and Soares, M. J. (2004) A prolactin family paralog regulates reproductive adaptations to a physiological stressor. *Proc. Natl. Acad. Sci. U.S.A.* **101,** 16543–16548